82721

# OXYGEN DIFFUSION IN CUPRATE SUPERCONDUCTORS*

J. L. Routbort

Materials Science Division

Argonne National Laboratory

Argonne, IL 60439-4838

and

S. J. Rothman

Journal of Applied Physics

Argonne, IL 60439-8296

Invited article to be submitted to *Applied Physics Reviews*.



*One of the authors (J.L.R.) was supported by the U.S. Department of Energy, BES-Materials Sciences under contract No. W-31-109-ENG.

Table of Contents

ABSTRACT

Superconducting properties of the cuprate superconductors depend on the oxygen content of the material; the diffusion of oxygen is thus an important process in the fabrication and application of these materials. In the present article, we review studies of the diffusion of oxygen in $La_{2-x}Sr_xCuO_4$, $YBa_2Cu_3O_{7-\delta}$, $YBa_2Cu_4O_8$, and the $Bi_2Sr_2Ca_{n-1}Cu_nO_{2n+4}$ (n = 1, and 2) superconductors, and attempt to elucidate the atomic mechanisms responsible.

## I. INTRODUCTION

The excitement caused by the discovery of the superconducting cuprates has calmed down into a steady development of their possible applications, e.g., as thin films in electronics or as silver-sheathed wires or tapes for current transmission. In addition to applications, research continues on their unusual structures and physical properties, along with a search for superconductivity in related compounds which may yield higher transition temperatures. Considerable efforts are directed towards microstructure refinement and development of modifications (texture, small second phases, dislocations, etc.) which could enhance flux pinning and thus yield higher critical current densities. One of the basic parameters that determine the superconducting properties of these compounds is the oxygen stoichiometry; in turn, oxygen stoichiometry is changed by the diffusion of

oxygen. Our interest, and the main thrust of this article, are the atomic mechanisms of oxygen diffusion in these compounds.

The mechanisms of diffusion are linked with the presence and behavior of point defects, so a brief summary of the defect chemistry of the cuprate superconductors is included in this review. At the risk of offending some of our esteemed colleagues, we have cited articles which we believe are illustrative rather than attempting to cite all of the relevant, but copious literature. We begin by describing the necessary fundamentals; in succeeding sections, we discuss diffusion and defects in the different supeconducting cuprates, $La_{2-x}Sr_xCuO_4$, $YBa_2Cu_3O_{7-\delta}$ (Y 1:2:3), $YBa_2Cu_4O_8$ (Y 1:2:4), and $Bi_2Sr_2Ca_{n-1}Cu_nO_{2n+4}$ (n = 1 and 2) (2:2:0:1 and 2:2:1:2).

## IA. The Diffusion Coefficient

In one dimension, diffusion obeys the diffusion equation:

$$\frac{\partial}{\partial x}\left(D\frac{\partial C}{\partial x}\right)=\frac{\partial C}{\partial t}, \qquad (1)$$

where $C$ is the concentration of the diffusing species, $x$ a space coordinate, $t$ the time of diffusion, and $D$ the diffusion coefficient. In this article, we are concerned with two kinds of diffusion coefficients, the chemical diffusion coefficient and the tracer diffusion coefficient. The chemical diffusion coefficient $\tilde{D}$ describes diffusion under a gradient of chemical potential and corresponds to an experiment in which a sample is equilibrated under a

certain oxygen partial pressure ($P_{O_2}$), the $P_{O_2}$ is changed, and the sample re-equilibrates to the new $P_{O_2}$ by the diffusion of oxygen. Therefore $\tilde{D}$ is the diffusion coefficient which describes oxygenation. Measurement of $\tilde{D}$ is usually carried out by measuring the time-dependence of some property (often the electrical resistivity) of the entire sample, (Fig. 1)[1] as the oxygen content equilibrates with the new $P_{O_2}$, calculating a relaxation time, $t$, and calculating the diffusion coefficient from $t$ with the use of a linear dimension $x$ over which the diffusion takes place, according to the equation

$$D = \frac{x^2}{6t} . \qquad (2)$$

The tracer diffusion coefficient $D^*$ describes diffusion in the absence of a gradient of chemical potential. In the corresponding experiment, a sample is equilibrated at $P_{O_2}$ in natural oxygen (0.002 $^{18}O$) and is then annealed at the same temperature and $P_{O_2}$, but in oxygen enriched to, say, 0.95 $^{18}O$. $D^*$ can be most accurately obtained[2] by depth profiling the $^{18}O$ with a secondary-ion mass spectrometer (SIMS) or by nuclear reaction analysis, and fitting the depth profile to the appropriate solution of eq. 1. Such a depth profile of in-diffused $^{18}O$ measured for diffusion in the c direction of a $Bi_2Sr_2CuO_x$ crystal annealed for 24 h at 550°C is shown in Fig. 2.[3] The open circles are the experimental points measured by SIMS and corrected for background while the solid line is the least-squares fit to the complementary error function solution to the diffusion equation, eq. 1. For more detailed descriptions of the experimental techniques, the reader is referred to the original papers.

The chemical and tracer diffusion coefficients are related by:

$$\tilde{D} = D^* (1+\partial \ln \gamma / \partial \ln c), \tag{3}$$

where the quantity in brackets on the right hand side is the thermodynamic factor with $\gamma$ the activity coefficient of the diffusant; this term takes account of the fact that the driving force in a chemical diffusion experiment is the gradient in the chemical potential, and not in the concentration.[4] In a highly nonideal substance like $YBa_2Cu_3O_{7-\delta}$, the value of the thermodynamic factor (Fig. 3)[5] may differ greatly from unity, and may depend strongly on temperature and stoichiometry. $D^*$ is most closely related to point defect properties and therefore is more directly correlated with atomic transport mechanisms than is $\tilde{D}$ because it does not contain the thermodynamic factor. We shall use $D$ to refer to both kinds of diffusion coefficients when the statement applies to both coefficients.

Another variant of eq. 2,

$$D = \Gamma x^2 f/6, \tag{4}$$

where $\Gamma$ is the jump frequency of the diffusing atoms and $f$ the Bardeen-Herring correlation factor,[6] (neglected in this discussion) suggests that the diffusion coefficient can be obtained from a measurement of $\Gamma$, for instance by internal friction.[7]

$D$ is a second-rank tensor,[8] and thus has two values for tetragonal crystals (one parallel and one perpendicular to the four-fold or $c$ axis) or three for crystals of orthorhombic symmetry, one parallel to each principal crystallographic axis. This is an important point because in the case of highly anisotropic crystal structures, such as the cuprates, enormous differences between the values of the diffusion coefficients in the different crystal directions can be expected. Further, when measuring $D$ on a polycrystalline sample, some averaging takes place. In a SIMS experiment, $C$ (eq. 1) is averaged over the different grains included in the analyzed area (typically 10 μm diameter), which leads to complications in the analysis of the depth profiles,[9] and an unexpectedly large scatter in the results, as the orientations of the analyzed grains are not controlled. It is clearly preferable to make measurements on single crystals, but that also involves serious experimental problems.[10]

## IB. Point Defects

Atomic transport usually takes place via the motion of point defects (as opposed to a direct exchange of neighboring atoms), and is therefore connected to the thermodynamics of the defects through the concentration of the defects and the defect equilibria. All of the superconducting oxides are nonstoichiometric compounds whose deviation from stoichiometry is controlled by the defect equilibria. The defects include atomic defects on both the oxygen (usually the majority defect) and cation lattices and electronic

defects (electrons or holes). The latter, along with a mobility term, enter into the normal state electrical properties (conductivity, thermoelectric power, and Hall effect) and affect the critical transition temperature for the onset of superconductivity. The defect equilibria include $P_{O_2}$ and the temperature, T, the latter by way of the Arrhenius dependence of the equilibrium constants.

Typical defect equilibria are the incorporation of intersitital oxygen:

$$1/2\, O_2 \Leftrightarrow O_i'' + 2\dot{h}, \tag{5}$$

or the filling of oxygen vacancies:

$$\ddot{V}_O + 1/2\, O_2 \Leftrightarrow O_O + 2\dot{h} \tag{6}$$

where Kröger-Vink notation[11] is used.

## II. DIFFUSION IN $La_{2-x}Sr_xCuO_4$

### IIA. Point Defect Equilibria

The defects in pure $La_2CuO_4$ are electron holes and oxygen interstitials.[12-14] The electrical conductivity, $\sigma$, increases as $(P_{O_2})^{1/6}$ as expected from eq. 5. The conductivity at a given value of $P_{O_2}$ is independent of temperature, i. e., the enthalpy for the reaction in eq. 5 is zero. That oxygen enters the lattice interstitially has been confirmed by neutron diffraction studies on the isostructural compound $La_2NiO_4$.[15]

Discussion of a comprehensive defect equilibrium model for $La_{2-x}Sr_xCuO_4$ is beyond the scope of this review. Nevertheless if one combines eqns. 5 and 6 with intrinsic electronic disorder, e.g.

$$\text{null} \Leftrightarrow e' + \dot{h} \tag{7}$$

and intrinsic Frenkel disorder,

$$O_O^x \Leftrightarrow O_i'' + \ddot{V}_O, \tag{8}$$

the resulting charge neutrality equation for doubly charged oxygen vacancies and interstitials becomes:

$$n + 2[O_i''] + [Sr'_{La}] = p + 2[\ddot{V}_O] + [(Sr'_{La}, \ddot{V}_O)^{\cdot}] \tag{9}$$

where $n = [e']$, $p = [\dot{h}]$ and one allows for the formation of $(Sr'_{La}, \ddot{V}_O)^{\cdot}$ complexes.

At low concentrations of strontium $[Sr'_{La}]$, x = 0.05-0.1, the electrical conductivity is independent of $P_{O_2}$,[16] indicating that the strontium, which has a charge of -1 with respect to the $La^{+3}$ it substitutes for, is charge-compensated by electron holes and determines $p$, according to:

$$p = [Sr'_{La}]. \tag{10}$$

At still higher values of x, the strontium is charge-compensated by both oxygen vacancies and holes and

$$[Sr'_{La}] = p + 2[\ddot{V}_O]. \tag{11}$$

The change of the compensation mechanism is related to the peak in the plot of σ vs. $[Sr'_{La}]$ which is thought to be connected to the peak in $T_c$ as a function of $[Sr'_{La}]$, the phenomenon which made oxygen diffusion in $La_{2-x}Sr_xCuO_4$ interesting in the first place. Fig. 4 presents the $T_c$ vs. $[Sr'_{La}]$ data.[17] However, a decrease of $p$ with increasing $[Sr'_{La}]$ cannot be explained by simple defect theory and other factors have to be considered.[12,16] Also, the negatively charged $Sr'_{La}$ and the positively charged $\ddot{V}_O$ tend to associate, forming either a neutral or a singly charged complex, so that $\ddot{V}_O$ is a minority species.[16]

Measurements of the line-shape parameter for positron annihilation showed that this parameter remained constant for x = 0.05-0.15, but increased for x = 0.2.[18] We believe that $\ddot{V}_O$ would repel positrons and thus not affect the lineshape parameter. Therefore this increase represents, in our opinion, an increase in $[nSr'_{La}, \ddot{V}_O]$. A rough calculation shows that n = 2, i.e. two Sr ions complex with one $\ddot{V}_O$. Calculations based on this model[18] qualitatively reproduced the experimental peak in Tc, and the experimentally observed vacancy concentrations[19,20] (Fig. 5). The computer-calculated defect energies in $La_2CuO_4$ show a high formation energy[21] for isolated $\ddot{V}_O$, consistent with this picture.

## IIB. Tracer Diffusion

Two compatible sets of data on tracer diffusion of oxygen now exist: one on polycrystals with x = 0.10, 0.15, or 0.20[22] and one on c-direction single crystals with x = 0, 0.07, 0.09, and 0.12; the latter set also includes data on polycrystals with x=0.1[23](Fig. 6). The two sets of data agree reasonably well where they overlap given the possible reasons for scatter, e.g. phase purity, density, etc. For nearly the same values of x, $D^*$ in the polycrystals » $D_c^*$, indicating that $D^*$ in $La_{2-x}Sr_xCuO_4$ is highly anisotropic, because the $D^*$ measured on a randomly oriented grain is

$$D^*(\Theta) = D_c^* \cos^2\Theta + D_{ab}^* \sin^2\Theta, \qquad (12)$$

(where $D_c$ and $D_{ab}$ represent the diffusion coefficients parallel and perpendicular, respectively, to the *c* axis, which makes an angle Θ with the diffusion direction; see remarks above and ref. 10 for averaging in a SIMS measurement). The anisotropy, $D_{ab}/D_c \approx 600$ at 500°C in $La_{1.9}Sr_{0.1}CuO_4$.[23]

The variation of $D_c$ with x (Fig. 7)[23] at low x can be explained by the change from diffusion via oxygen interstitials only at x = 0 to diffusion via interstitials and Sr-introduced $\ddot{V}_O$ at x = 0.03. $D_c$ at x = 0.07 is three orders of magnitude lower than for x = 0 and continues to fall as x increases, and similar behavior is found for polycrystals.[22] It was reported that $D$ was "very rapid" for x = 0 and 0.05 which was attributed to open porosity.[22] In light of the single crystal results, the large $D$ may have simply been the consequence

of the large variation in $D$ with x. Opila et al.[23] suggest that ordering of the oxygen ion vacancies is responsible for this very rapid drop, whereas Smedskjaer et al.,[18] motivated by the positron annihilation results, suggest formation of $\ddot{V}_O$-$2Sr'_{La}$ complexes. The two explanations may be reconciled by saying that the complexes order. The drop in $D^*$ is strikingly similar to the decrease of oxygen ion conductivity with dopant concentration in $ZrO_2$ and $CeO_2$.[24]

## III. DIFFUSION IN $YBa_2Cu_3O_{7-\delta}$

### IIIA. Structure and point defects

To understand the peculiarities of diffusion in $YBa_2Cu_3O_{7-\delta}$, its structure must first be understood. The Cu and O atoms in the well-known orthorhombic $YBa_2Cu_3O_{7-\delta}$ structure (Fig. 8)[25] are arranged in the $CuO_2$ planes (O(2) and O(3), Cu(2)) and the CuO chains (Cu(1) and O(1)), with additional oxygens around the $Ba^{++}$ ions (O(4)). When the structure is ordered ($\delta = 0$), the O(1) sites are fully occupied and the O(5) sites are empty (the OI structure).[26] As $\delta$ increases, due to increasing temperature or decreasing $P_{O_2}$, some O(1) sites become vacant. At higher temperatures, some O(5) sites are filled and a few O(4) sites also become vacant. At the orthorhombic-tetragonal transformation, an equal number of O(1) and O(5) sites are filled. It should be noted that in the orthorhombic phase, the vast majority of the $\ddot{V}_O$ are located on O(1). The influence of oxygen stoichiometry

on $T_c$ in Y 1:2:3 (Fig. 9)[27] is even more spectacular than in $La_{2-x}Sr_xCuO_4$, but the defect structure is different. Oxygen vacancies are introduced not by doping with aliovalent cations, but by changing the temperature or oxygen partial pressure, and the charge of the $[\ddot{V}_O]$ is compensated by changes in the hole concentration.[28]

The $\ddot{V}_O$ are distributed on O(1) sites randomly only when $\delta$ is close to 0 (Fig. 10A).[29] When $\delta$ is finite, the $\ddot{V}_O$ tend to align themselves in strings[26] because the Cu ions on either side of a $\ddot{V}_O$ are three-fold coordinated, an energetically unfavorable configuration.[30] In other words, the number of string ends is minimized. What is more, the full and empty strings also order; at $\delta = 0.5$, alternate rows of O(1) sites are full or empty (Fig. 10B). This configuration is responsible for the plateau in $T_c$ at 60K (Fig. 9). Calculations show that the oxygen ions in the tetragonal phase also line up in (probably short) strings, but the strings occur with equal probability along either the *a* or *b* directions (Fig. 10C). Phase diagrams corresponding to these configurations have been calculated by several groups, see e.g. ref. 26.

These structural peculiarities manifest themselves in the defect thermodynamics. When measurements of the non-stoichiometry, $\delta$, as a function of the temperature and oxygen partial pressure[5,30-34] are fitted to one of several proposed models of the defect structure,[30,32,35] the value of the enthalpy of oxidation for the equilibrium constant in the mass action equation corresponding to the defect equilbrium (eq. 6)

$$[O_o]\, p^2/[\ddot{V}_O] = K_{ox}\,(P_{O_2})^{0.5} \qquad (13)$$

turns out to be more or less independent of $\delta$, except very close to $\delta = 0$, and so does the thermodynamic factor (eq. 3).[5] This is an unexpected result in view of the fact that this is a highly non-ideal system; the explanation of Hong et al.[30] is that only the oxygen ions at the end of a chain are mobile, and the number of chain ends is not a strong function of $P_{O_2}$ as changes in $P_{O_2}$ are accomodated by changes in the chain length.

### IIIB. Theory

Many of the theories of the diffusion of oxygen in Y 1:2:3 are based on the correlated motion of single vacancies in the *ab* plane. (Everyone agrees that diffusion in the *c* direction is much slower.) Because of the ordering of the vacancies, we believe that this mechanism is likely to be operative only at very low values of $\delta$. We therefore believe that calculations of the diffusion coefficient based on this model [36-38] are not representative of what is really going on in this system. This is also indicated by the disagreement of these theories with some of the trends in the experimental data (see below).[10] Nevertheless, the theories are worth reviewing.

The tracer diffusion coefficient of oxygen in Y 1:2:3 calculated[37] from a thermodynamic model which in turn was based on two energy parameters calculated from the temperature dependence of the oxygen site occupancy[28,37] showed a slight $P_{O_2}$ dependence and a break at the orthorhombic-tetragonal transformation. Addition of a Monte Carlo calculation of the Bardeen-Herring correlation factor [36] yielded somewhat

lower values of the diffusion coefficient, but did not change the qualitative aspects of the variation of the diffusion coefficient with $P_{O_2}$ or temperature.

Calculation of tracer and chemical diffusion coefficients by Monte Carlo simulations of an asymmetric next-nearest-neighbor Ising model yielded a strongly stoichiometry-dependent value of D which also displayed significant anisotropy in the *ab* plane.[38] A lattice gas model qualitatively reproduced the oxygen ordering in the *ab*-plane, but no diffusion coefficients were calculated.[39] A calculation of oxygen tracer diffusion coefficients using the cluster variation method in conjunction with the path probability method yielded activation energies of 77 and 116 kJ/mol in the tetragonal and orthorhombic phases, respectively, with a stoichiometry-dependent $D$, and a break in the Arrhenius plot at the orthorhombic-tetragonal transformation.[40] A migration energy of 29 kJ/mol has been calculated for oxygen ions using a shell model and associated two-and three-body short-range interaction potentials.[41] In another model,[42] it was assumed that the force between two neighboring oxygen ions was repulsive for an O(1) and O(5) site, repulsive for two O(1) sites in the $a$ direction and attractive in the $b$ direction. A strong anisotropy of the diffusion coefficient in the $ab$ plane and a strong stoichiometry dependence of the diffusion coefficient were obtained.

Calculations on the path of the jumping atom have also been carried out. One calculation[43] showed that vacancy diffusion via the O(1)-O(4)-O(1) path was energetically the most favorable. A recent computer simulation, based on energy minization procedures and the Mott-Littleton methodology,

attributed diffusion to vacancy migration between O(1) sites, not directly, but via O(5) or O(4) sites.[44] The calculated migration energy was 95.5 kJ/mole.

One model,[45] not based on the assumption that oxygen diffusion occurs via the correlated motion of single vacancies suggested that oxygen could move interstitially over the O(5) sites (along channels parallel to the *b*-direction) with an almost zero activation energy for motion. A mean field calculation[45] gave activation energies for diffusion in the *a* and *c* directions ≈ 164 kJ/mol. Strictly speaking, this is not diffusion via an interstitial, but rather a model in which an oxygen ion moves along a row of vacant sites (O(5)). Clearly no universally accepted theory of oxygen diffusion in Y 1:2:3 is available.

There have been a number of attempts to model the electrical properties. The model of Su, et al.[35] used disproportionation of the Cu into multivalent and univalent sites, the oxidation reaction, and assumed small polaron conduction to describe the conductivity and thermopower. On the other hand, the model of Maier and Tuller[46] used partially ionized and/or neutral interstitial oxygen defects and $YBa_2Cu_3O_6$ as the reference composition to sucessfully describe the observed $P_{O_2}$ and T dependences of the conductivities, thermopower, and the oxygen nonstoichiometry. The Maier and Tuller model seems more applicable to highly nonstoichiometric Y 1:2:3 because it accounts for high defect concentrations, but both models give reasonable agreement with the measured conductivities. It is fair to state that much more theoretical and experimental work must be performed

before there exists an unambigious and universally accepted point defect model for Y 1:2:3.

### IIIC. Chemical Diffusion

Most investigations of the diffusion of oxygen in Y 1:2:3 have been carried out under a gradient of oxygen chemical potential and have therefore measured chemical diffusion. These measurements are very important technologically and if properly performed and interpreted can aid elucidation of the atomic diffusion mechanisms. The most recent investigations[1,47,48] include experiments on the concentration dependence of $\tilde{D}$ and discuss the atomic diffusion mechanism. These authors have performed a careful investigation of the change of electrical resistance during isothermal in-diffusion as a function of the initial oxygen content from 650 to 708°C and as a function of $P_{O_2}$ from 450°C - 850°C. Their results indicate that $\tilde{D}$ is a function of $\delta$, increasing as $\delta$ increases, a result which is not in accord with earlier thermogravimetric measurements performed in the temperature range of 550 to 850°C.[49] Earlier measurements of the electrical resistivity changes reported[42] activation energies for oxygen in-diffusion, of 48 and 125 kJ/mol for $\delta$ equal to 0.38 and 0, respectively. This result suggested that $\tilde{D}$ increased with increasing $\delta$, consistent with the results of La Graff and Payne.[1] The earlier work of Tu, et al.[42] also reported a difference in the activation energy for oxygen chemical diffusion between in- and out-diffusion. However, O'Sullivan and Chang[50] found no differences in $\tilde{D}$ for

in- and out-diffusion determined from solid-state electrochemical measurements.

The references cited here are but a few of the many, and often conflicting, reports of oxygen chemical diffusion in Y 1:2:3. Part of the scatter probably arises from the variation in sample properties, particularly density, stoichiometry, and impurity concentration, and partially is the result of the analysis which requires assuming a diffusion distance. This is usually taken as the sample dimensions, or as the grain size. If the sample has connected porosity, the former assumption can lead to values of $\tilde{D}$ which are four to six orders of magnitude too high. Nevertheless, values of $\tilde{D}$ are always much larger that the oxygen tracer diffusivity, as expected from the magnitude of the thermodynamic factor (Fig. 3.).

### IIID. Tracer diffusion in single crystals

Single crystals of Y 1:2:3 are usually very small platelets with the largest face parallel to the $ab$ plane. The dimension along the $c$ axis is at best a few hundred microns. The as grown crystals are invariably twinned; in order to measure $D_a$ and $D_b$ separately, the crystals first have to be de-twinned. This is accomplished by squeezing gently in the $a$ direction at 400°C.[51] Measurement of $D_c$ with SIMS is relatively easy; measurements in the $ab$ plane involve either coming in with the SIMS beam from the edge of a thin crystal, a very delicate operation, or taking a series of two-dimensional $^{18}O$ images as a function of depth.

Measurements of the diffusion of oxygen in 123 single crystals[10,52,53] (Fig. 11) have shown that:

1. Diffusion is anisotropic, with $D_c \ll D_{ab}$. The ratio can be as large as $10^6$ at $\approx$ 400°C, but decreases with increasing temperature since the activation energy for diffusion in the *c* direction is larger ($\approx$ 200 kJ/mole) than in the *ab* plane (93.6 kJ/mole).

2. SIMS profiles on a de-twinned crystal (Fig. 12) show that diffusion in the *ab* plane is highly anistropic at 300°C and $P_{O_2} = 10^5$ Pa, i.e., at low $\delta$, with $D_b \gg D_a$.[10] In this instance, $D_a$ is too small to be calculated from the depth profile. Other values of $D_a$ (crosses in Fig. 11) are scattered because the crystal retwinned during annealing. However, the elegant SIMS imaging measurements of Tsukui, et al.[53] indicate that the anisotropy no longer exists i.e. $D_b \approx D_a$, at 600°C and $P_{O_2} = 2 \times 10^4$ Pa (high $\delta$).

Other interesting features of the data are:

1. $D_{poly} \approx D_{ab}$. This is not unexpected; if the grains are randomly oriented, $D_{poly}$ is obtained by the intergration of eq 12:

$$D_{poly} \approx D_{ab} \langle \sin^2\Theta \rangle = \frac{2}{3} D_{ab}, \qquad (14)$$

where the average is taken over a hemisphere.

2. At 300°C, $D_b \approx 10\ D_{ab}$. This can be understood by following the path of a diffusing atom in a twinned and in a de-twinned crystal with $D_b \gg D_a$ (Fig.13). In a given time, both atoms take the same number of jumps, but in the de-twinned crystal, all of these are in the direction of the analyzing beam

and thus contribute to diffusion, whereas in the twinned crystal, only $N_b$ jumps are in the direction of the analyzing beam and $N_a$ do not contribute to diffusion. Then $D_b / D_{ab} = (N_a + N_b)/N_b \approx (\Sigma A^2 + \Sigma B^2)/\Sigma B^2$, where the A's and B's are the thicknesses of the twins with the $a$ (striped in Fig. 13) or $b$ axis parallel to the diffusion direction. This leads to $D_b > D_{ab}$ by a factor that depends on the twin thickness.

3. The data for $D_c$ are scattered over several orders of magnitude. This is a result of different degrees of misorientation in the crystals, giving rise to different levels of contributions from diffusion in the $ab$ plane. (Consider eq. 12, with $D_{ab} \gg D_c$,, $D_{ab}/D_c \geq (\Theta)^{-2}$, $\Theta$ very small, and scattered at random). The lowest observed value is thus the upper limit for $D_c$.

### IIIE. Tracer diffusion in polycrystalline $YBa_2Cu_3O_{7-\delta}$

A value of 146 kJ/mol has been obtained for the activation energy for oxygen diffusion in Y 1:2:3 in the temperature range 377-812°C from measurements of the oxygen ion conductivity,[54] in principle a measurement of tracer diffusion. The conductivity was measured by a complex impedance technique, using yttria stabilized $ZrO_2$ (YSZ) electrodes that were blocking for the electron or hole current, but transparent to the oxygen ion current. We are not sure of the validity of this measurement, since the transference number for electrons in YSZ appears to be greater than the transference number for oxygen ions in Y 1:2:3.[55]

The tracer diffusion of oxygen has been measured by following the exchange of $^{18}O$ in the atmosphere with $^{16}O$ in powder in situ with a microbalance.[56] The results were reported as $D$ = 0.287 exp (-198.5 kJ/mol/RT) $cm^2/s$ for anneals under $P_{O_2}$ = 6.5 x $10^3$ Pa. Problems were encountered at low temperatures with a rate-limiting surface reaction. It is not clear how a diffusion coefficient can be obtained from an integral measurement under these conditions. A measurement such as this would clearly measure the fastest component of the diffusion tensor.

The tracer diffusion of oxygen in polycrystalline Y 1:2:3 has been measured using the SIMS technique over a temperature range of 300°C to 850°C, $P_{O_2}$ = $10^5$ Pa (points in Fig. 14)[9] and between 300 and 650°C at the same $P_{O_2}$ on polycrystalline samples whose grain sizes varied (solid line in Fig. 14).[57] These values of $D$ were obtained from penetration plots fit to the sum of two complementary error functions, representing a "fast" and a "slow" diffusion coefficient. These terms correspond to the presence of more than one grain in the analysis area, with different values of $D$ because of the large anisotropy of diffusion. The larger diffusion coefficient represented diffusion in a direction closer to the $ab$–plane.[9] The agreement between the two investigations is reasonable, especially in light of the complications of anisotropy and possible variations in composition and/or amount of second phase present in the samples. Some variation of $D$ with phase purity has also been noted.[9] The oxygen diffusivity in more phase-pure samples can be described by an Arrhenius relation[9] given by,

$$D = 1.4 \times 10^{-4} \exp [-(93.6 \text{ (kJ/mole)}/RT] \text{ cm}^2/\text{s}. \quad (15)$$

In addition to the temperature dependence, the dependence of $D$ on $P_{O_2}$ can provide valuable insight on the diffusion mechanism. Eq. 6 predicts that $[V_O]$ should vary as $(P_{O_2})^{-1/m}$, where m depends on the charge of the $V_O$ and how it is compensated; it generally ranges between 2 and 6. Measurements of the $P_{O_2}$ dependence at 400°C[10] and 600°C[9] carried out over as wide a $P_{O_2}$ range as possible without decomposition (Fig. 15), indicate that to within an experimental uncertainty of about a factor of 2, $D$ is independent of $P_{O_2}$. This fact strongly suggests that oxygen diffusion does not take place via an oxygen vacancy mechanism as proposed by Bakker, et al.[37] or Tu, et al.[42] It should be admitted that if m were equal to 6, the variation of $D$ expected from eqn. 6 over two orders of magnitude in $P_{O_2}$ would be approximately equal to the experimental uncertainty.

### IIIF. The Mechanism of Oxygen Diffusion in Y 1:2:3

The experimental facts that any diffusion mechanism must be consistent with are:

1. $D^*$ is independent of or only weakly dependent on $P_{O_2}$.
2. The Arrhenius plot for $P_{O_2} = 10^5$ Pa is straight over the entire temperature range, with no break at the orthorhombic-tetragonal transformation.
3. $D_b \gg D_a$ at low values of $\delta$ (300°C and $P_{O_2} = 10^5$ Pa) but $D_b \approx D_a$ at higher values of $\delta$ (600°C and $P_{O_2} = 2 \times 10^4$ Pa).

4. $D_c \ll D_{ab}$ at low temperatures, the activation energy and the preexponential factor, $D_o$, for the $c$ direction are much higher than for the $ab$ plane.

The first of these results suggests that $D$ is nearly independent of $[V_O]$ and $[O_i]$. The second suggests that the same jump is responsible for diffusion in the orthorhombic and tetragonal phases. The third suggests that the relative magnitudes of $D_a$ and $D_b$ depend on the number of rows of oxygen ions in each direction in the $ab$ plane; this suggests that diffusion takes place parallel to the chains in the $ab$ plane. $D$ for such a mechanism would show a weak dependence on $P_{O_2}$ because only the oxygen ions at the ends of the chains are mobile and the number of chain ends depends only weakly on $P_{O_2}$. We suggested the following atomic mechanism of oxygen diffusion in the $ab$ plane of Y 1:2:3: oxygen ions break loose from the chain ends, diffuse parallel to the chains, and pop into a vacant chain-end site (Fig. 16). The detailed diffusion path cannot be deduced from these experimental results, but it seems likely that the diffusion takes place over the empty sites parallel to the chain. This heuristic idea is not supported by many of the calculations mentioned in the section on theory.

Diffusion in the $c$ direction appears more likely to take place over individual lattice vacancies; this is suggested both by the higher values of $D_o$ and the activation energy.

## IIIG. Internal Friction and Diffusion

Many investigators have measured internal friction,[7,58-66] anelastic relaxation,[67-69] or relaxation of $T_c$[70,71] in Y 1:2:3. Most of the internal friction peaks are not related to diffusion,[58] but the internal friction peak whose shape and position depend on oxygen partial pressure, and which appears at 210K at 1.18 Hz and shifts to 800K for 40 kHz, is generally attributed to oxygen ions hopping between the non-equivalent O(1) and O(5) sites as the result of the applied stress, i.e. a reorientation of elastic dipoles. The frequencies corresponding to the internal friction peaks, or to anelastic relaxation, or relaxation of $T_c$ (Fig.17) fall on a reasonably good Arrhenius line, with an activation energy of 110.0 ± 1.1 kJ/mol.[67] The approximate agreement with the activation energy for self-diffusion of oxygen in polycrystalline Y 1:2:3 (93.6 ± 2.9 kJ/mol) suggests that the same jump might be responsible for the internal friction as for the long-range diffusion of oxygen.

The fact that the activation energy for internal friction and the anelastic relaxation measurements is higher than that of tracer diffusion has been ascribed to the fact that the internal friction involves a spectrum of activation energies reflecting the local environment, whereas diffusion involves the lowest energy jumps.[67] However, in general, the diffusion coefficients calculated from internal friction measurements using a dipole reorientation model are about a factor of three lower than those obtained from direct tracer measurements.[7] It should also be pointed out that the internal friction peaks do not have an ideal Debye shape.

Very recently Tallon and Mellander[72] have observed that the temperature at which the internal friction peak occurs in $RBa_2Cu_3O_{7-\delta}$ (R = Gd, Nd, and La) at 40 kHz shifts systematically to lower temperatures as the radius of the R cation increases from Y to La. They suggested that the shift is the result of a large enhancement in oxygen mobility, 19, 48, and 97 times for Gd, Nd, and La, respectively which results from the replacement of the smaller Y ions with a larger ion. Neutron diffraction studies of $NdBa_2Cu_3O_{7-\delta}$ (Nd 1:2:3) for $0.09 < \delta < 0.74$[73] indicate that the repulsive energy between oxygen ions on the O(1) and the O(5) site is lower in Nd-1:2:3 than in Y 1:2:3, 12 kJ/mol compared to 19 kJ/mol. Therefore, one might expect that the activation energy for oxygen self-diffusion would be lower, resulting in faster oxygen diffusion in Nd 1:2:3 compared to Y 1:2:3. A lower repulsion energy could also decrease the internal friction relaxation time, and hence at a fixed frequency, shift the internal friction peak to lower temperature.

Oxygen tracer diffusion measurements in Nd 1:2:3, however, do not exhibit the predicted enhancement.[74] Within experimental uncertainty, the oxygen diffusion coefficients are the same in Y 1:2:3 and Nd 1:2:3 (Fig. 18). The reasons for the disagreement between the tracer and the internal friction measurements are not clear, but the simple relationships between internal friction and oxygen diffusion must be questioned. It is possible that the substitution of Nd for Y changes other factors which compensate an expected change in the diffusion coefficient,[74] or even that the internal friction peak is the result of O(2) to O(3) exchanges, as suggested by Zhang, et al.[65]

It seems evident that the relationship between oxygen diffusion internal friction is not completely uncertain. On the one hand, the agreement between the activation energies and the absolute values of the diffusion coefficient is reasonable. On the other hand, internal friction peaks shift with substitution[72] and show curved Arrhenius plots and a $D$ which depends on $P_{O_2}$,[62] neither of which is consistent with direct oxygen tracer diffusion measurements. Further diffusion studies on other systems, accompanied by simulation calculations could provide an answer.

## IV. DIFFUSION IN $YBa_2Cu_4O_8$

$YBa_2Cu_4O_8$ is a high-temperature superconductor with $T_c \approx 80K$. The Y 1:2:4 structure differs from the Y 1:2:3 in two important respects. First, Y 1:2:4 has a double Cu-O chain,[75] as opposed to the single Cu-O chain in Y 1:2:3. The Y 1:2:4 unit cell can be considered as two Y 1:2:3 cells joined chain-to chain with the second cell displaced b/2 along the b axis.[75] Second, the Y 1:2:4 compound does not deviate nearly as much from the stoichiometric composition as the Y 1:2:3 because each oxygen of the double chain is bonded to three copper cations rather than to two.[75] In order to explore the effect of these differences on diffusion, oxygen tracer diffusion was measured in Y 1:2:4 polycrystals between 400 and 700°C in $P_{O_2}$ that varied between $10^3$ and $10^5$ Pa and in the $c$ direction of Y 1:2:4 single crystals at 600 and 700°C for $P_{O_2} = 10^5$ Pa.[76]

The oxygen diffusion coefficient in Y 1:2:4 depends strongly on $P_{O_2}$ (Fig. 19). The data follows the proportionality, $D \propto (P_{O_2})^{-0.7 \pm 0.2}$, in contrast to the diffusion in Y 1:2:3, which is not a strong function of $P_{O_2}$ ($D \propto (P_{O_2})^{0 \pm 0.15}$). This result is sufficient to conclude that the oxygen tracer diffusion occurs via different mechanisms in Y 1:2:3 and Y 1:2:4. Oxygen vacancies are indicated for Y 1:2:4. In fact, if the oxygen vacancies were neutral of if the hole concentration were fixed, eq. 6 would predict a -0.5 $P_{O_2}$ dependence, about equal, within experimental uncertainty, to the measured exponent.

The Arrhenius plots for oxygen diffusion in Y 1:2:4 and Y 1:2:3 (Fig. 20) also indicate a difference in mechanism. The activation energy and $D_o$ for the Y 1:2:4 polycrystals

$$D_{poly} = 0.08 \exp [-(200.6 \text{ kJ/mole})/RT] \text{ cm}^2/\text{s} \qquad (16)$$

are much higher than for Y 1:2:3 (eq. 12). Additionally, a preexponential of 1 $cm^2/s$ is predicted for vacancy diffusion in metals[77] and 0.08 is certainly closer to 1 than is $1.4 \times 10^{-4}$ $cm^2/s$ (eq. 15). An oxygen vacancy diffusion mechanism is also consistent with high-temperature measurements of conductivity and Seebeck coefficient.[78] The simulation studies for oxygen diffusion in Y 1:2:4 by Islam and Baetzold,[44] using the same potentials as those used for the Y 1:2:3,[41] yield a Q of 203 kJ/mole for vacancy diffusion with motion from an O(1) to an O(5). The calculated value of 203 is remarkably close to the experimentally measured value of 200.6 kJ/mole.

We believe that these results are consistent with the motion of oxygen ions over vacant O(5) sites, proposed as the mechanism for oxygen diffusion in Y 1:2:3, in that the activation energy, Q, for Y 1:2:3 would only reflect the formation energy, but Q for Y 1:2:4 would contain both formation and migration energies and hence be approximately twice the Q in Y 1:2:3, as observed.

The Arrhenius plot of Fig. 21 exhibits the expected anisotropy in that diffusion along the *c* direction in Y 1:2:4:

$$D_c = 75 \exp [-(296 \text{ kJ/mole})/RT] \text{ cm}^2/\text{s} \qquad (17)$$

is slower than diffusion in the polycrystals, which therefore represents diffusion in the *ab* plane. It is expected that the formation of nonchain oxygen vacancies is more difficult and, in addition, long-range diffusion in the *c* direction involves long jump distances and motion through Cu-O, Ba-O, and Y planes. The anisotropy between diffusion in the *c* direction and in the *ab* plane is less in Y 1:2:4 than in Y 1:2:3 because the additional migration energy term required for Y 1:2:4 means that diffusion in the *ab* plane of Y 1:2:4 will always be much less than diffusion in the *ab* plane of Y 1:2:3.

Thus, the oxygen tracer diffusion results on Y 1:2:4 indicate that the diffusion mechanism is different than in Y 1:2:3, and likely to involve an oxygen ion vacancy mechanism. The results in Y 1:2:4 are also consistent with the proposed model for oxygen diffusion in Y 1:2:3.

## V. DIFFUSION IN $Bi_2Sr_2CuO_x$ and $Bi_2Sr_2CaCu_2O_x$

The $Bi_2Sr_2Ca_{n-1}Cu_nO_{2n+4}$ system contains three superconducting compounds: 2:2:0:1 (n = 1), 2:2:1:2 (n = 2), and 2:2:2:3 (n = 3). The structure of these compounds is shown in Fig. 21. The basic 10-K 2:2:0:1 structure consists of the layer sequence of Bi-O, Sr-O, Cu-O, Sr-O, and Bi-O stacked along the c axis. The Cu-O layer is replaced by a three-layer Cu-O, Ca, Cu-O sequence ($CuO_2$) in the 85-K 2:2:1:2 and is replaced by two $CuO_2$ sequences in the 110-K 2:2:2:3.[79] The c lattice parameters are 24.6, 30.7, and 37.1 Å for 2:2:0:1, 2:2:1:2, and 2:2:2:3, respectively. The structures undergo an incommensurate modulation[80] thought by some to be due to interstitial oxygen atoms located in the Bi-O plane.

It is surprising that so little diffusion data for these superconductors exists since relatively large single crystals and phase pure polycrystalline 2:2:0:1 and 2:2:1:2 are available, but not phase-pure, high-density 2:2:2:3. The change of resistance of 2:2:1:2 single crystal with oxygen content has been used to measure $\tilde{D}$.[81] In-diffusion was found to be significantly faster than out-diffusion; the same result that was found for Y 1:2:3. A $\tilde{D}$ was calculated and found equal to

$$\tilde{D} = 11.7 \exp[(-112 \text{ kJ/mole})/RT], \text{ cm}^2/\text{s} \qquad (18)$$

which represents diffusion in the *ab* plane.[81] Li, et al.[82] investigated $\tilde{D}$ in 2:2:1:2 single crystals using a thermograviometric technique. They reported

that for out-diffusion $\tilde{D}$ = 6.1 x $10^{-8}$ $cm^2/s$ at 500°C, about five times slower than given in eq. 18. They also found that diffusion in the *ab* plane was anisotropic with $\tilde{D}_a / \tilde{D}_b \geq 5\text{-}6$.[82] An internal friction peak was observed at low frequencies ($10^{-2}$ – 5 Hz) in the temperature range of 300 – 420K in a BSCCO superconductor whose composition before sintering was $BiSrCaCu_2O_x$. It was speculated that the relaxation, characterized by an activation energy of ≈ 110 kJ/mole, was the result of the migration of oxygen along the *c* axis.[83] One measurement on the mechanical aftereffect in $Bi_{1.8}Pb_{0.4}Sr_2Ca_{2.2}Cu_3O_y$ has been made; an activation energy of 85.9 kJ/mole can be calculated based on an attempt frequency of $10^{13}$/s.[69]

A few speculations concerning tracer diffusion based on the structure can now be made. The structure of the *ab* planes of the three compounds are the same and all undergo an incommensurate modulation. Therefore, it is likely that diffusion in the *ab* plane of all three superconductors will be the same. Diffusion parallel to the *c* direction is likely to be a difficult process and one would expect a large anisotropy between diffusion parallel to *c* and in the *ab* plane.

Oxygen tracer diffusion measurements confirm these predictions. Diffusion in the *ab* plane of 2:2:0:1: single crystals and in 2:2:1:2 polycrystals falls on the same Arrhenius line to high precision (Fig. 22).[3,84] Comparison of the $D$ values in Fig. 22 with diffusion along the c axes of 2:2:0:1 and 2:2:1:2 (Fig. 23) confirms the expected anisotropy $D_{ab} \gg D_c$, hence $D_{poly} \approx D_{ab}$ for 2:2:1:2.

Diffusion in 2:2:1:2 polycrystals is described by the Arrhenius relation:

$$D = 1.7 \times 10^{-5} \exp [-(89.7 \text{ kJ/mole})/RT] \text{ cm}^2/\text{s}. \quad (19)$$

The parameters contrast with those for diffusion along the *c* axis:

$$D_c^{2:2:0:1} = 0.06 \exp [-(203.6 \text{ kJ/mole})/RT] \text{ cm}^2/\text{s} \quad (20)$$

and

$$D_c^{2:2:1:2} = 0.6 \exp [-(212.3 \text{ kJ/mole})/RT] \text{ cm}^2/\text{s}, \quad (21)$$

and the same conclusions in regard to mechanisms can be drawn as for Y 1:2:3.

The diffusion behavior for the 2:2:1:2 polycrystals is quite similar to that in Y 1:2:3 (Fig. 22), and the similarity extends to the close compatibility with the activation energy calculated from mechanical aftereffect.[69] Additionally, the preexponential factor of $1.7 \times 10^{-5}$ cm$^2$/s is closer to what one might expect for interstitial diffusion than to the 1 cm$^2$/s expected for vacancy diffusion.[77] The values of the parameters for diffusion in the 2:2:1:2 polycrystals support the idea that oxygen diffuses in the *ab* plane of $Bi_2Sr_2Ca_{n-1}Cu_nO_{2+n}$ via an interstitial mechanism, consistent with the idea that the incommensurate modulations in the Bi-O planes are caused by oxygen interstitials.

On the other hand, the activation energy for diffusion along the *c* axis is more than twice as large as for diffusion in the polycrystals, and the preexponential factors are quite close to the Zener value quoted above,

suggesting that diffusion of oxygen along the $c$ axis in 2:2:0:1 and 2:2:1:2 takes place via vacancies.

Why the values of $D_c$ for the two compounds differ by only a factor of 4, even though the 2:2:1:2 contains a Ca plane and a Cu-O plane not found in the 2:2:0:1, is not obvious. The activation barrier is nearly the same for the $c$ direction jump in the two compounds, indicating that the activation barrier occurs between similar pairs of planes in the two compounds. It seems reasonable to assume that there is one activation barrier, i.e., one interplanar jump, that is rate controlling. The jump distance is therefore equal to the $c$ lattice parameter, so that the square of the jump distance, which is a factor in the preexponential, is 1.6 times greater for 2:2:1:2 than for 2:2:0:1. The source of the additional factor of 2.5 is unknown.

## VI. SUMMARY

Oxygen tracer diffusion measurements have yielded a plethora of fundamental information on atomic transport mechanisms in high-temperature superconductors, especially in $YBa_2Cu_3O_{7-\delta}$. Diffusion in all of the superconductors is highly anisotropic, reflecting the structure. However, despite the importance of the diffusion of oxygen on superconducting properties, there remain several areas of concern which will require more work. In particular, the lack of simulations to explain all of the experimental features of oxygen tracer diffusion in $YBa_2Cu_3O_{7-\delta}$ is disconcerting. In addition, the relationship between internal friction and

oxygen diffusion appears to be in doubt and will need further experimental and theoretical investigations. It would seem that a possible experimental approach would be an investigation of tracer diffusion in the RE–substituted 1:2:3 compounds.

There are some results on the BSCCO superconductors, namely 2:2:0:1 and 2:2:1:2, but no oxygen diffusion results on the 2:2:2:3 superconductor. These superconductors as well as the Tl– and Hg–based superconductors will require extensive experimental studies, before any theoretical advancements can be made and tested.

**Acknowledgements**

None of the tracer diffusion experiments would have been possible without the expertise of J. E. Baker who operates the SIMS at the Center for the Microanalysis of Materials at the University of Illinois, Urbana. We thank Ms Baker for her skill and dedication and the Center for their hospitality. The authors are grateful to a host of colleagues who have collaborated with us in the experiments, provided samples, sent us preprints, and/or given us permission to use their figures in this review. Some of the most prominent, but not all, of these are R. Baetzold, N. Chen, J. R. Cost, B. Dabrowski, P. Dalman, B.K. Flandermeyer, D. De Fontaine, K.C. Goretta, Th. Hehenkamp, J. R. LaGraff, J.-Z. Li, T. O. Mason, J. N. Mundy, L.J. Nowicki, M. Runde, L.C. Smedskjaer, J.L. Tallon, U. Welp, R. K. Williams, C.L. Wiley, and X. Xu.

One of the authors (J. L. R.) acknowledges the support of the United States Department of Energy, Basic Energy Sciences-Materials Science, under Contract No. W-31-109-ENG-38.

## REFERENCES


[1]J. A. LaGraff and D. A. Payne, Physica C **212**, 478 (1993).

[2]S. J. Rothman, J. L. Routbort, J. E. Baker, L. J. Nowicki, K. C. Goretta, L. J. Thompson and J. N. Mundy, *Diffusion Analysis and Applications*, A. D. Romig and M. A. Dayananda, eds. (The Minerals, Metals & Materials Society, Warrendale, PA, 1989) pp. 289-305.

[3]M. Runde, J. L. Routbort, J. N. Mundy, S. J. Rothman, C. L. Wiley and X. Xu, Phys. Rev. B **46**, 3142 (1992).

[4]L. Darken, AIME **174**, 184 (1948).

[5]F. Faupel and T. Hehenkamp, Z. Metallkd. **84**, 529 (1993).

[6]J. Bardeen and C. Herring, *Atom Movements* J. H. Holloman, ed. (American Society for Metals, Cleveland, 1951) p. 87.

[7]J. R. Cost and J. T. Stanley, J. Mater. Res. **6**, 232 (1991).

[8]J. F. Nye, *The Physical Properties of Crystals* (Oxford University Press, Oxford, 1957) p. 23.

[9]S. J. Rothman, J. L. Routbort and J. E. Baker, Phys. Rev. B **40**, 8852 (1989).

[10]S. J. Rothman, J. L. Routbort, U. Welp and J. E. Baker, Phys. Rev. B. **44**, 2326 (1991).

[11]F. A. Kröger, *The Chemistry of Imperfect Crystals* (Wiley, New York, 1964) pp. 1001-1002.

[12]D. J. L. Hong and D. M. Smyth, J. Sol. Stat. Chem. **97**, 427 (1992).

[13]E. J. Opila, G. Pfundtner, J. Maier, H. L. Tuller and B. J. Wuench, Mater. Sci. Eng. B **13**, 165 (1992).

[14]M.-Y. Su, E. A. Cooper, C. E. Elsbernd and T. O. Mason, J. Am. Ceram. Soc. 73, 3453 (1990).

[15]J. D. Jorgensen, B. Dabrowski, S. Pei, D. R. Richards and D. G. Hinks, Phys. Rev. B **40**, 2187 (1989).

[16]L. Shen, P. A. Salvador and T. O. Mason, J. Am. Ceram. Soc. **77**, 81 (1994).

[17]M. W. Shafer, T. Penny and B. L. Olson, Phys. Rev. B **36**, 4047 (1987).

[18]L. C. Smedskjaer, J. L. Routbort, B. K. Flandermeyer, S. J. Rothman, D. G. Legnini and J. E. Baker, Phy. Rev. B **36**, 3903 (1987).

[19]N. Nguyen, J. Choisnet, M. Hervieu and B. Raveau, J. Solid State Chem. **39**, 120 (1981).

[20]D. G. Hinks, B. Dabrowski, K. Zhang, C. U. Segre, J. D. Jorgensen, L. Soderholm and M. A. Beno, Mat. Res. Soc. Symp. Proc. **99**, 9 (1988).

[21]M. S. Islam, M. Leslie, S. M. Tomlinson and C. R. A. Catlow, J. Phys. C **21**, L109 (1988).

[22]J. L. Routbort, S. J. Rothman, B. K. Flandermeyer, L. J. Nowicki and J. E. Baker, J. Mater. Res. **3**, 116 (1988).

[23]E. J. Opila, H. L. Tuller and B. J. Wuench, J. Am. Ceram. Soc. **76**, 2363 (1993).

[24]A. S. Nowick, in *Diffusion in Crystalline Solids* , eds. G. E. Murch and A. S. Nowick, (Academic Press, New York, 1984) pp. 143-188.

[25]J. D. Jorgensen, M. A. Beno, D. G. Hinks, L. Soderholm, K. J. Volin, R. L. Hitterman, J. D. Grace, I. K. Schuller, C. U. Segre, K. Zhang and M. S. Kleefisch, Phys. Rev. B **36**, 3708 (1987).

[26]G. Ceder, M. Asta, M. Carter, D. de Fontaine, M. E. Mann and M. Sluiter, Phys. Rev. B **41**, 8698 (1990).

[27]R. Liu, B. W. Veal, A. P. Paulikas, J. W. Downey, H. Shi, C. G. Olson, C. Gu, A. J. Arko and J. J. Joyce, Phys. Rev. B **45**, 5614 (1992).

[28]H. Shaked, J. D. Jorgensen, J. Faber Jr., D. G. Hinks and B. Dabrowski, Phys. Rev. B **39**, 7363 (1989).

[29]M. Asta, D. de Fontaine, G. Ceder, E. Salomons and M. Kraitchman, J. Less Common Metals **168**, 39 (1991).

[30]D. J. L. Hong, A. Mehta, P. Peng and D. M. Smyth, Ceram. Trans. **13**, 129 (1990).

[31]K. Kishio, T. Hasegawa, K. Suzuki, K. Kitazawa and K. Fueki, Mat. Res. Soc. Symp. Proc. **156**, 91 (1989).

[32]L. A. Andreev, Y. S. Nechaev, E. A. Kalashnikova, N. T. Konovalov, V. A. Lykhin, Y. A. Minaev and N. A. Olshevskii, Phys. Stat. Sol. B **163**, 221 (1991).

[33]P. K. Gallagher, Adv. Ceramic Materials **2**, 632 (1987).

[34]T. B. Lindemer, J. F. Hunley, J. E. Gates, A. L. Sutton Jr., J. Brynestad, H. C.R. and P. K. Gallagher, J. Am. Ceram. Soc. **72**, 1775 (1989).

[35]M.-Y. Su, S. E. Dorris and T. O. Mason, J. Solid State Chem. **75**, 381 (1988).

[36]H. Bakker, J. P. A. Westerfeld and D. O. Welch, Physica C **153-155**, 848 (1988).

[37]H. Bakker, J. P. A. Westerveld, D. M. R. Do Cascio and D. O. Welch, Physica C **157**, 25 (1989).

[38]E. Salomons and D. de Fontaine, Phys. Rev. B **41**, 11159 (1990).

[39]Z. X. Cai and S. D. Mahanti, Solid State Commun. **67**, 287 (1988).

[40]J. S. Choi, M. Sarikaya, I. A. Aksay and R. Kikuchi, Phys. Rev. B **42**, 4244 (1990).

[41]R. C. Baetzold, Phys. Rev. B **42**, 56 (1990).

[42]K. N. Tu, N. C. Yeh, S. I. Park and C. C. Tsuei, Phys. Rev. B **39**, 304 (1989).

[43]M. S. Islam, Supercond. Sci. Technol. **3**, 531 (1990).

[44]M. S. Islam and R. C. Baetzold, J. Mater. Chem. **in press**, (1994).

[45]M. Ronay and P. Nordlander, Physica C **153-155**, 834 (1988).

[46]J. Maier and H. L. Tuller, Phys. Rev. B **47**, 8105 (1993).

[47]J. R. LaGraff and D. A. Payne, Physica C **212**, 470 (1993).

[48]J. A. LaGraff and D. A. Payne, Physica C **212**, 487 (1993).

[49]K. Kishio, K. Suzuki, T. Hasegawa, T. Yamamoto and K. Kitazawa, J. Sol. State Chem. **82**, 192 (1989).

[50]E. J. M. O'Sullivan and B. P. Chang, Appl. Phys. Lett. **52**, 1441 (1988).

[51]U. Welp, M. Grimsditch, H. You, W. K. Kwok, M. M. Fang, G. W. Crabtree and J.-Z. Liu, Physica C. **161**, 1 (1989).

[52]S. I. Bredikhin, G. S. Emel'chenko, V. S. Shecktman, A. A. Zhokhov, S. Carter, R. J. Carter, J. A. Kilner and B. C. H. Steele, Physica C 286 (1991).

[53]S. Tsukui, T. Yamamoto, M. Adachi, T. Oka, Y. Shono, K. Kawabata, N. Fukoka, A. Yanase, Y. Yoshioka and F. Tojo, Defect and Diffusion Forum 1123 (1993).

[54]D. J. Vischjager, P. J. Van Der Put, J. Schram and J. Schoonman, Solid State Ionics **27**, 199 (1988).

[55]L. Heyne and N. M. Beeckmans, Proc. Brit. Ceram. Soc. **19**, 229 (1971).

[56]Y. Ikuma and S. Akiyoshi, J. Appl. Phys. **64**, 3915 (1988).

[57]J. Sabras, C. Colin, J. Ayache, C. Monty, R. Maury and A. Fert, Coll. de Phys. **51**, C1 (1990).

[58]B. S. Berry, W. C. Pritchet and T. M. Shaw, Defect and Diffusion Forum **75**, 34 (1991).

[59]E. Bonetti, E. G. Campari, P. Cammarota, A. Casagrande and S. Mantovani, J. Less Common Metals **164-5**, 231 (1990).

[60]G. Canelli, R. Canelli, F. Cordero, F. Trequattrini, S. Ferraro and M. Ferretti, Solid State Comm. **80**, 715 (1991).

[61]J. L. Tallon, A. H. Schuitema and N. E. Tapp, Appl. Phys. Lett. **52**, 507 (1988).

[62]J. L. Tallon and M. P. Staines, J. Appl. Phys. **68**, 3998 (1990).

[63]J. Woirgard, A. Riviere, P. Gadaud and P. Tal, Europhys. Lett. **17**, 601 (1992).

[64]X. M. Xie, T. G. Chen and Z. L. Wu, Phys. Rev. B. **40**, 4549 (1989).

[65]J. X. Zhang, G. M. Lin, Z. C. Lin, K. F. Liang, P. C. W. Fung and G. G. Siu, J. Phys.:Cond. Matter **1**, 6939 (1989).

[66]J. X. Zhang, G. M. Lin, W. G. Zeng, K. F. Liang, Z. C. Lin, G. G. Siu, M. J. Stokes and P. C. W. Fung, Supercond. Sci. and Technol. **3**, 163 (1990).

[67]J. R. Cost and J. T. Stanley, Scripta Metall. et Mater. **28**, 773 (1993).

[68]J. R. Cost, P. E. Armstrong, R. B. Poeppel and J. T. Stanley, Mater. Res. Soc. Proc. **209**, 819 (1991).

[69]T. Turner, Private Communication (1990).

[70]B. W. Veal, A. P. Paulikas, H. You, H. Shi, Y. Fang and J. W. Downey, Phy. Rev. B **42**, 4770 (1990).

[71]B. W. Veal, A. P. Paulikas, H. You, H. Shi, Y. Fang and J. W. Downey, Phys. Rev. B **42**, 6305 (1990).

[72]J. L. Tallon and B.-E. Mellander, Science **258**, 781 (1992).

[73]H. Shaked, B. W. Veal, J. Faber Jr., R. L. Hitterman, U. Balachandran, G. Tomlins, H. Shi, L. Morss and A. P. Paulikas, Phys. Rev. B **41**, 4173 (1990).

[74]J. L. Routbort, Physica C **124**, 408 (1993).

[75]P. Marsh, R. M. Fleming, M. L. Mandich, A. M. DeSantolo, J. Kwo, M. Hong and L. J. Martinez-Miranda, Nature **334**, 141 (1988).

[76]J. L. Routbort, S. J. Rothman, J. N. Mundy, J. E. Baker, B. Dabrowski and R. K. Williams, Phys. Rev. B **48**, 7505 (1993).

[77]C. Zener, J. Appl. Phys. **22**, 372 (1951).

[78]B.-S. Hong and T. O. Mason, Solid State Ionics **49**, 3 (1991).

[79]J. M. Tarascon, W. R. McKinnon, P. Barboux, C. M. Hwang, B. G. Bagley, L. H. Greene, G. W. Hull, Y. LePage, N. Stoffel and M. Giroud, Phys. Rev. B **38**, 8885 (1988).

[80]H. W. Zanderbergen, W. A. Groen, F. C. Mijlhoff, G. van Tendeloo and S. Amelinckx, Physica C **156**, 325 (1988).

[81]S. McKernan and A. Zettl, Physica C **209**, 585 (1993).

[82]T. W. Li, P. H. Kes, W. T. Fu, A. A. Menovsky and J. J. M. Franse, Physica C (1994).

[83]W. G. Zeng, P. C. W. Fung, G. M. Lin, J. X. Zhang, G. G. Siu, Z. L. Du and K. F. Liang, Solid State Comm. **71**, 949 (1989).

[84]M. Runde, J. L. Routbort, S. J. Rothman, K. C. Goretta, J. N. Mundy, X. Xu and J. E. Baker, Phys. Rev. B **45**, 7375 (1992).

## Figure Captions

Figure 1. Time–dependent electrical resistance for a $YBa_2Cu_3O_{7-\delta}$ single crystal during oxygen out–diffusion between 100% oxygen and increasingly lower oxygen partial pressures (from ref. 1).

Figure 2. Penetration plot obtained along the *c* direction of a $Ba_2Sr_2CuO_x$ sample annealed at 550°C for 24 h. The solid line is the least-squares fit to the complementary error function solution of the diffusion equation.[3]

Figure 3. Variation of the thermodynamic factor for $YBa_2Cu_3O_{6+x}$, points were measured at various temperatures, dotted line is theory.[5]

Figure 4. Variation of $T_c$ with concentration of Sr in $La_{2-x}Sr_xCuO_4$.[17]

Figure 5. Plot of oxygen vacancy concentration in $La_{2-x}Sr_xCuO_4$ vs. x. The line is calculated from the model of Smedskjær,[18] the squares from neutron diffraction,[20] and the circles from thermogravimetric analysis.[19]

Figure 6. Arrhenius plots for the diffusion of oxygen in $La_{2-x}Sr_xCuO_4$. S indicates diffusion in the c direction in single crystals,[23] P indicates diffusion in polycrystals.[22]

Figure. 7. Variation of $D_c$ with x for $La_{2-x}Sr_xCuO_4$ at 600°C.[23]

Figure 8. Structure of $YBa_2Cu_3O_{7-\delta}$.

Figure 9. Transition temperatures vs oxygen stoichiometry for $YBa_2Cu_3O_x$ single crystals.[27]

Figures. 10. Structures of Y 1:2:3 computed from Monte Carlo simulations;[29] small filled circles denote copper ions, large filled circles denote oxygen ions, and open circles denote vacant sites. Top to bottom are: Fig. 10A, near the stoichiometric composition, Fig. 10B, the low-temperature orthorhombic phase with $\delta = 0.5$, and Fig. 10C, the high-temperature tetragonal phase.

Figure 11. Arrhenius plot for the diffusion of oxygen in $YBa_2Cu_3O_{7-x}$ at $P_{O_2} = 10^5$ Pa. Line: polycrystals.[9] Hollow squares: $D_{ab}$ in twinned crystals, hollow triangle: $D_b$, crosses: $D_a$, open circles: $D_c$.[10] Square with cross: $D_c$, filled squares: $D_{ab}$.[52] Filled triangle: $D_c$, filled diamond: $D_a$ and $D_b$.[53]

Figure 12. Counts for $^{16}O$ and $^{18}O$ for both *a*– and *b*–directions in untwinned $YBa_2Cu_3O_{7-\delta}$ single crystals annealed 0.5 h at 300°C.[10]

Figure 13. Diffusion in untwinned and twinned areas. White: *b* vertical, shaded: *b* horizontal. The total length of the two lines is the same.

Figure 14. Arrhenius plot for the diffusion of oxygen in $YBa_2Cu_3O_{7-\delta}$ polycrystals (circles from ref. 9, line from ref. 57).

Figure 15 Variation of *D* in $YBa_2Cu_3O_{7-\delta}$ polycrystals vs. oxygen partial pressure at 400 and 600°C.[10]

Figure 16. Schematic sketch of proposed diffusion mechanism for oxygen in $YBa_2Cu_3O_{6.8}$. Open circles – oxygen, Closed circles– copper.

Figure 17. Relaxation time obtained from internal friction, anelastic relaxation, and time-dependent $T_c$ measurements vs 1/T. Data are from: filled circles,[62] crosses,[65] filled squares,[66] open triangles,[58] filled triangles,[7] open squares,[64] small filled square,[59] square cross,[70,71] and open circles.[69] The line is the fit to 26 data points from an anelastic relaxation experiment.[68]

Figure 18. Arrhenius plot of the oxygen tracer diffusion coefficient measured in Nd-123 (open circles) compared to that obtained for Y-123 (solid line).[74]

Figure 19. Variation of $D$ at 500°C (circles) and 600°C (triangles) with oxygen partial pressure for $YBa_2Cu_4O_8$.[76]

Figure 20. Arrhenius plot of oxygen diffusion data measured for polycrystalline Y 1:2:4 (circles)[76] and c-axis single crystals (triangles)[76] compared to polycrystaline Y 1:2:3.[9]

Figure 21. Structure of $Bi_2Sr_2Ca_{n-1}Cu_nO_{2n+4}$ for 2:2:0:1 (n =1), 2:2:1:2 (n = 2), and 2:2:2:3 (n = 3).

Figure 22 Arrhenius plot of the diffusion coefficients from oxygen tracer diffusion in polycrystalline $Bi_2Sr_2CaCu_2O_x$ (open circles),[84] compared to Y 1:2:3 polycrystals,[9] and parallel to the ab-plane in $Bi_2Sr_2CuO_x$ (crosses).[3]

Figure 23. Arrhenius plot showing oxygen diffusion in the c direction in $Bi_2Sr_2CaCu_2O_x$ (triangles) and $Bi_2Sr_2CuO_x$ (circles) compared to diffusion in polycrystalline $Bi_2Sr_2CaCu_2O_x$ (solid line).[3,84]

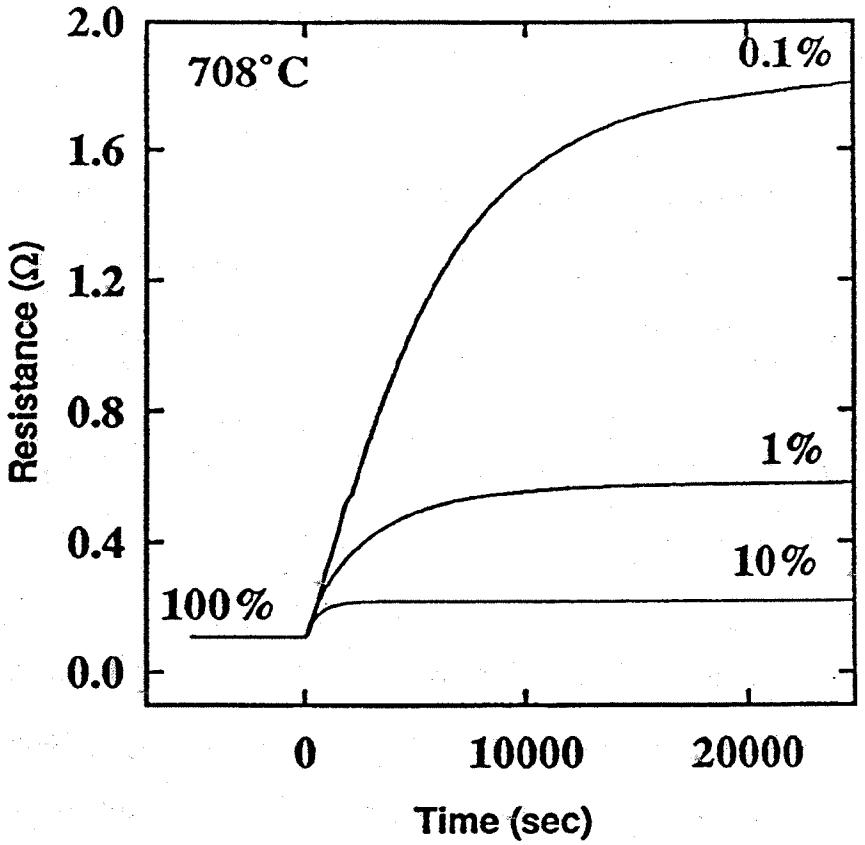


Figure 1. Time–dependent electrical resistance for a $YBa_2Cu_3O_{7-\delta}$ single crystal during oxygen out–diffusion between 100% oxygen and increasingly lower oxygen partial pressures (from ref 1).

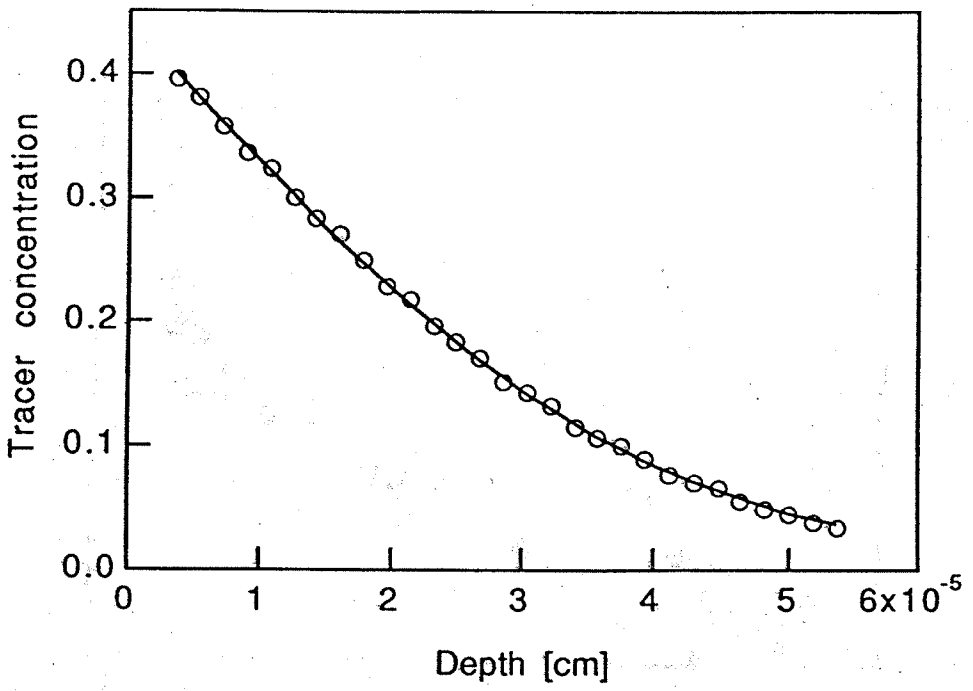


Figure 2. Penetration plot obtained along the *c* direction of a $Ba_2Sr_2CuO_x$ sample annealed at 550°C for 24 h. The solid line is the least-squares fit to the complementary error function solution of the diffusion equation.[3]

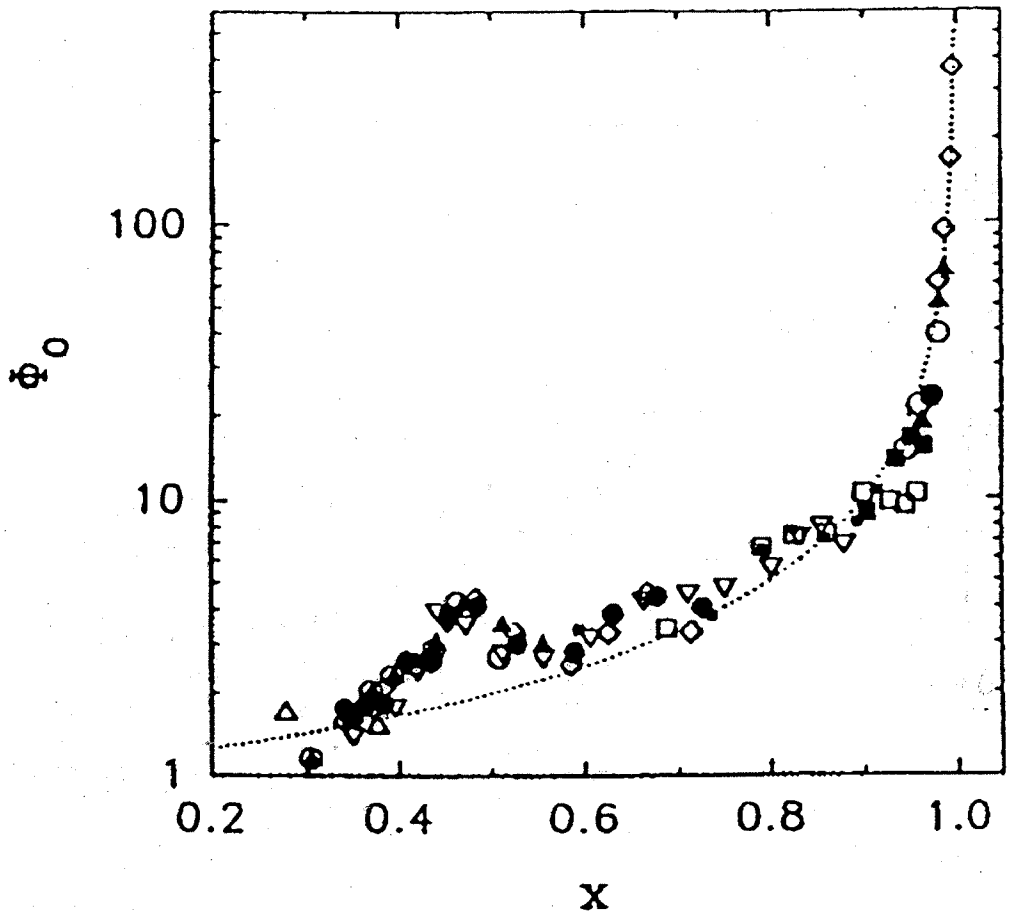


Figure 3. Variation of the thermodynamic factor for $YBa_2Cu_3O_{6+x}$, points were measured at various temperaures, dotted line is theory.[5]

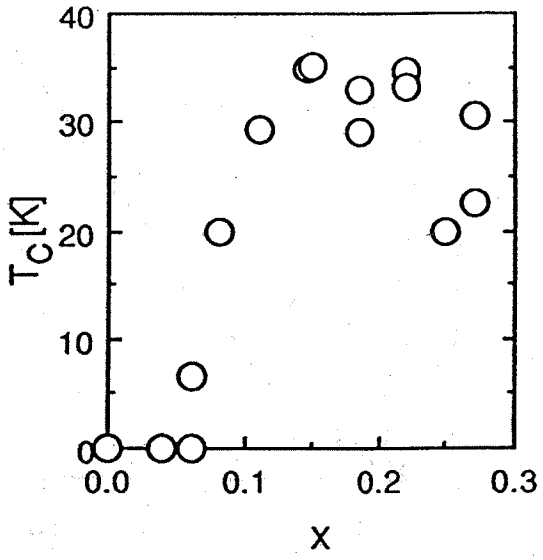


Figure 4. Variation of $T_c$ with concentration of Sr in $La_{2-x}Sr_xCuO_4$.[17]

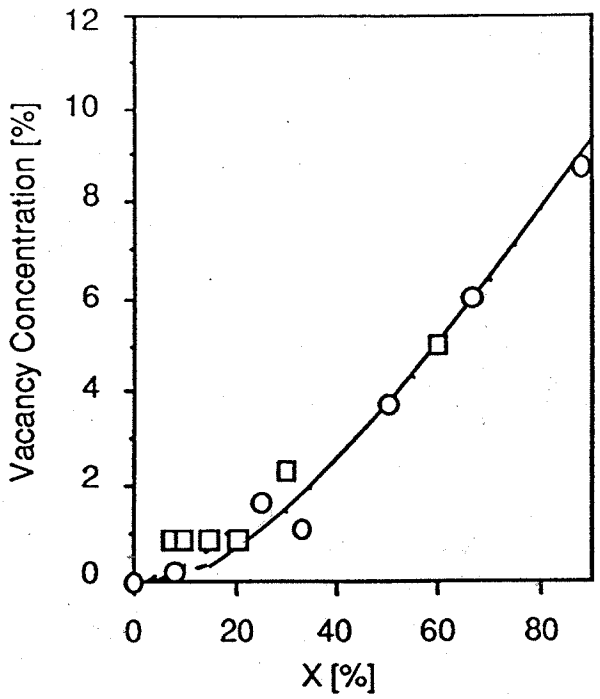


Figure 5. Plot of oxygen vacancy concentration in $La_{2-x}Sr_xCuO_4$ vs. x. The line is calculated from the model of Smedskjær,[18] the squares from neutron diffraction,[20] and the circles from thermogravimetric analysis.[19]

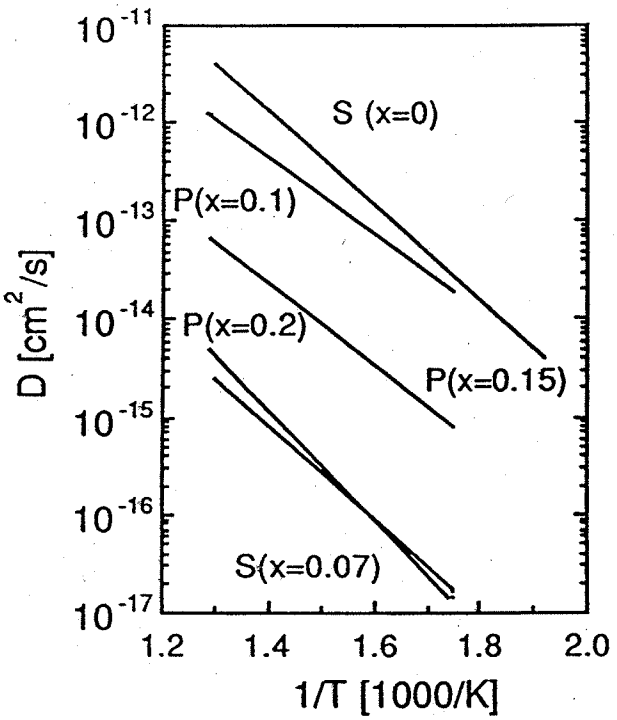


Figure 6. Arrhenius plots for the diffusion of oxygen in $La_{2-x}Sr_xCuO_4$. S indicates diffusion in the c direction in single crystals,[23] P indicates diffusion in polycrystals.[22]

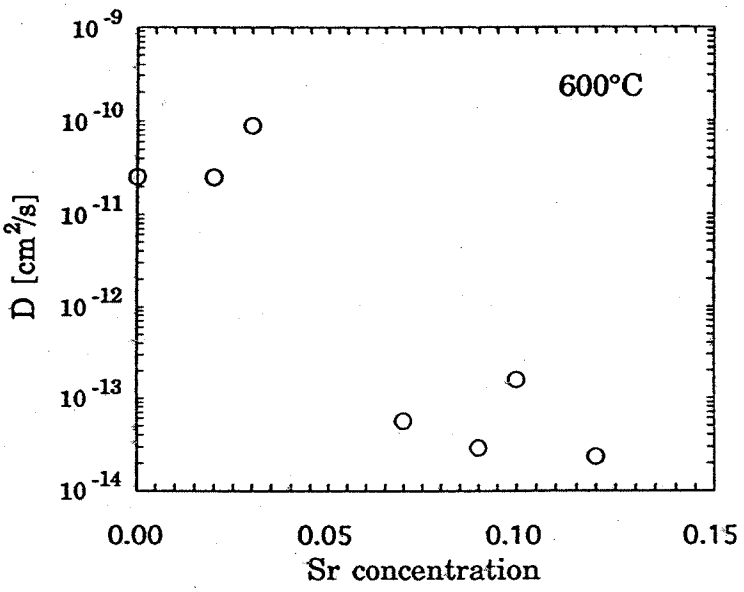


Figure. 7. Variation of $D_c$ with x for $La_{2-x}Sr_xCuO_4$ at 600°C.[23]

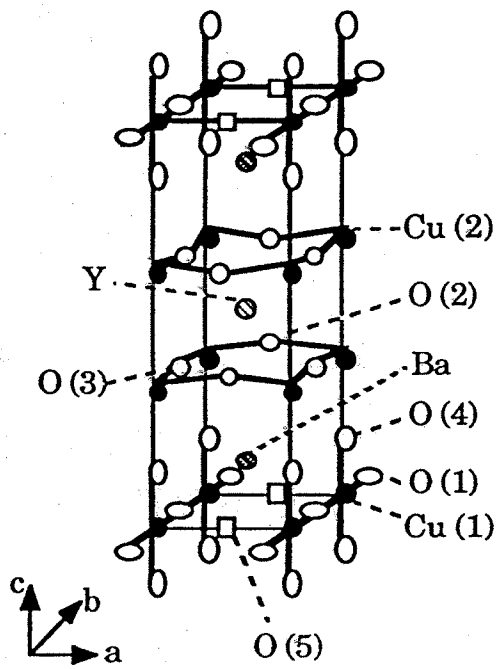


Figure 8. Structure of $YBa_2Cu_3O_{7-\delta}$.

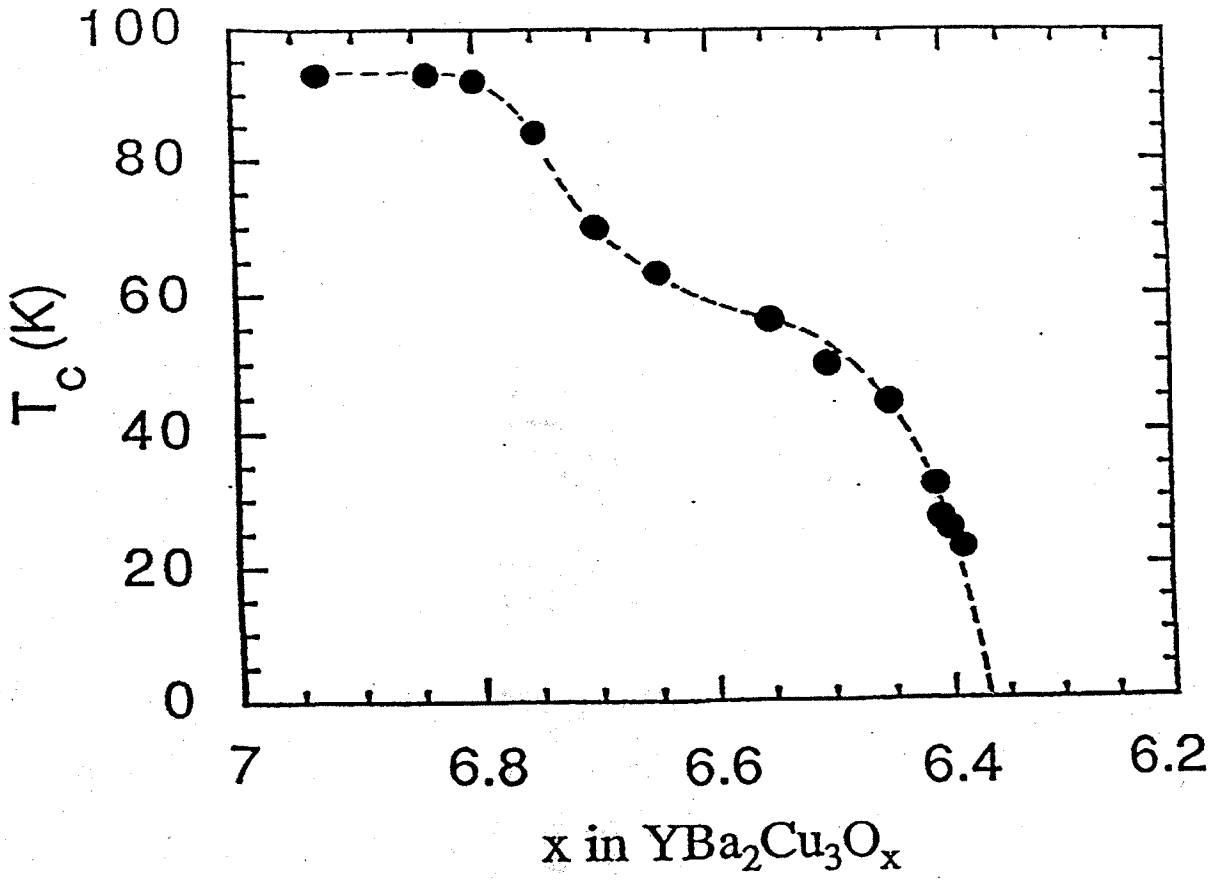


Figure 9. Transition temperatures vs oxygen stoichiometry for $YBa_2Cu_3O_x$ single crystals.[27]

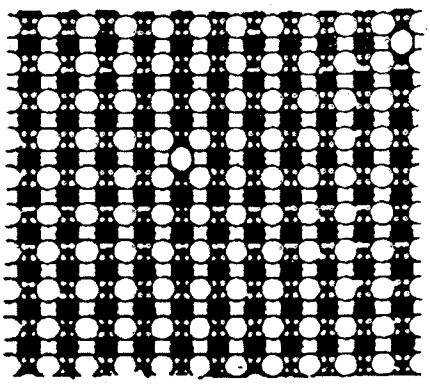

10A

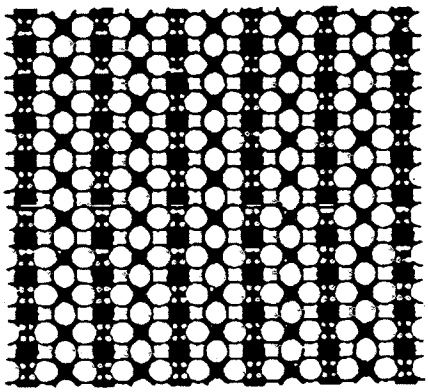

10B

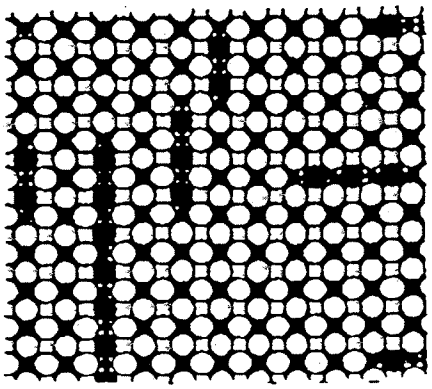

10C

Figures. 10. Structures of Y 1:2:3 computed from Monte Carlo simulations;[29] small filled circles denote copper ions, large filled circles denote oxygen ions, and open circles denote vacant sites. Top to bottom are: Fig. 10A, near the stoichiometric composition, Fig. 10B, the low-temperature orthorhombic phase with $\delta = 0.5$, and Fig. 10C, the high-temperature tetragonal phase.

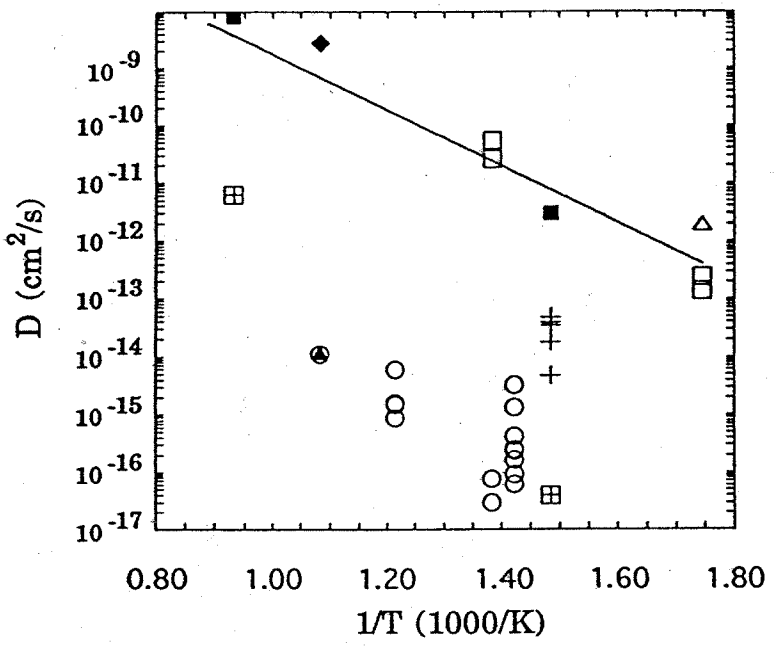


Figure 11. Arrhenius plot for the diffusion of oxygen in $YBa_2Cu_3O_{7-x}$ at $P_{O_2}$ = $10^5$ Pa. Line: polycrystals.[9] Hollow squares: $D_{ab}$ in twinned crystals, hollow triangle: $D_b$, crosses: $D_a$, open circles: $D_c$.[10] Square with cross: $D_c$, filled squares: $D_{ab}$.[52] Filled triangle: $D_c$, filled diamond: $D_a$ and $D_b$.[53]

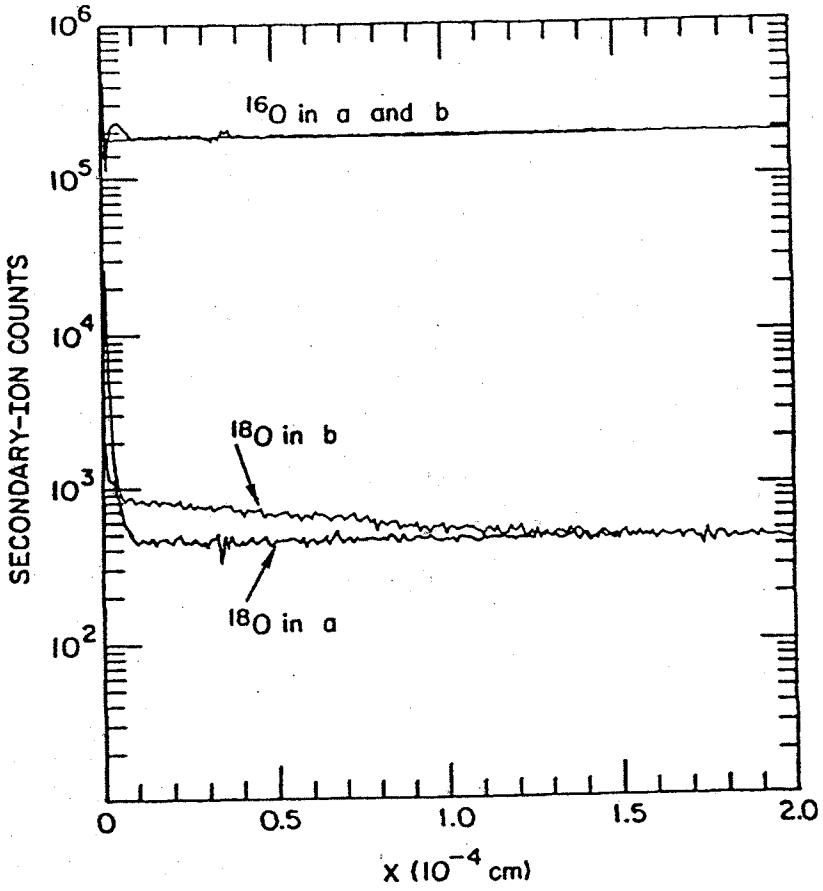


Figure 12. Counts for $^{16}O$ and $^{18}O$ for both *a*– and *b*–directions in untwinned $YBa_2Cu_3O_{7-\delta}$ single crystals annealed 0.5 h at 300°C.[10]

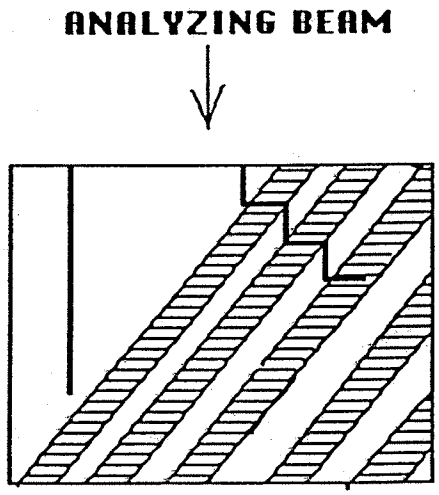


Figure 13. Diffusion in untwinned and twinned areas. White: *b* vertical, shaded: *b* horizontal. The total length of the two lines is the same.

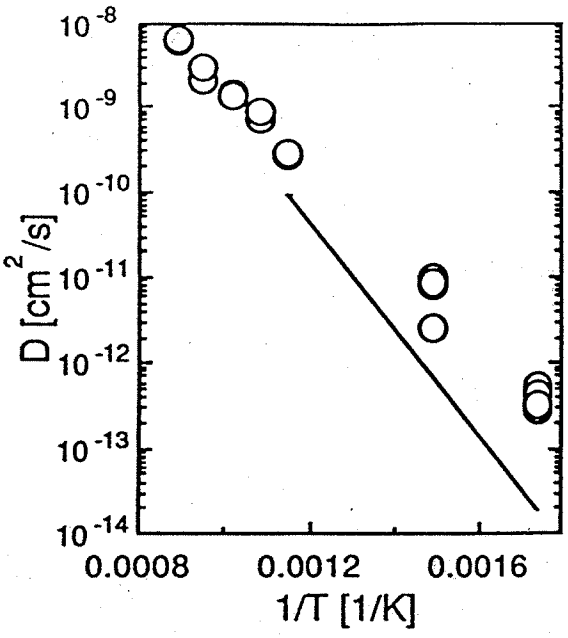


Figure 14. Arrhenius plot for the diffusion of oxygen in $YBa_2Cu_3O_{7-\delta}$ polycrystals (circles from ref. 9, line from ref. 57).

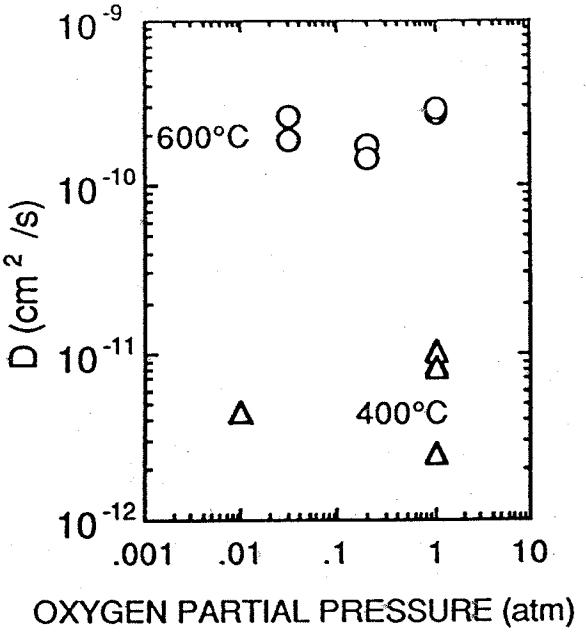


Figure 15 Variation of D in $YBa_2Cu_3O_{7-\delta}$ polycrystals vs. oxygen partial pressure at 400 and 600°C.[10]

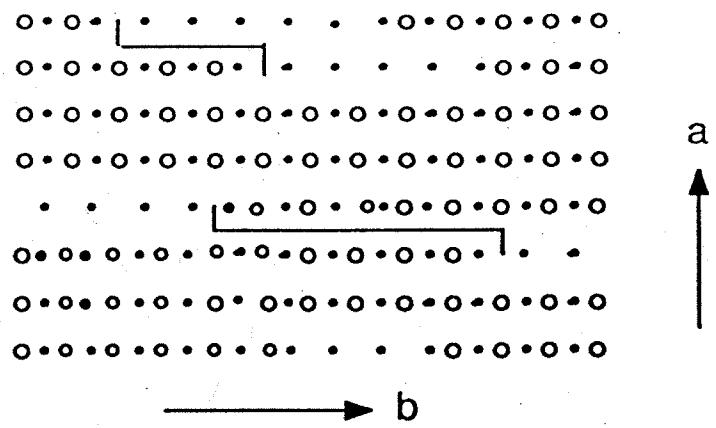


Figure 16. Schematic sketch of proposed diffusion mechanism for oxygen in $YBa_2Cu_3O_{6.8}$. Open circles – oxygen, Closed circles– copper.

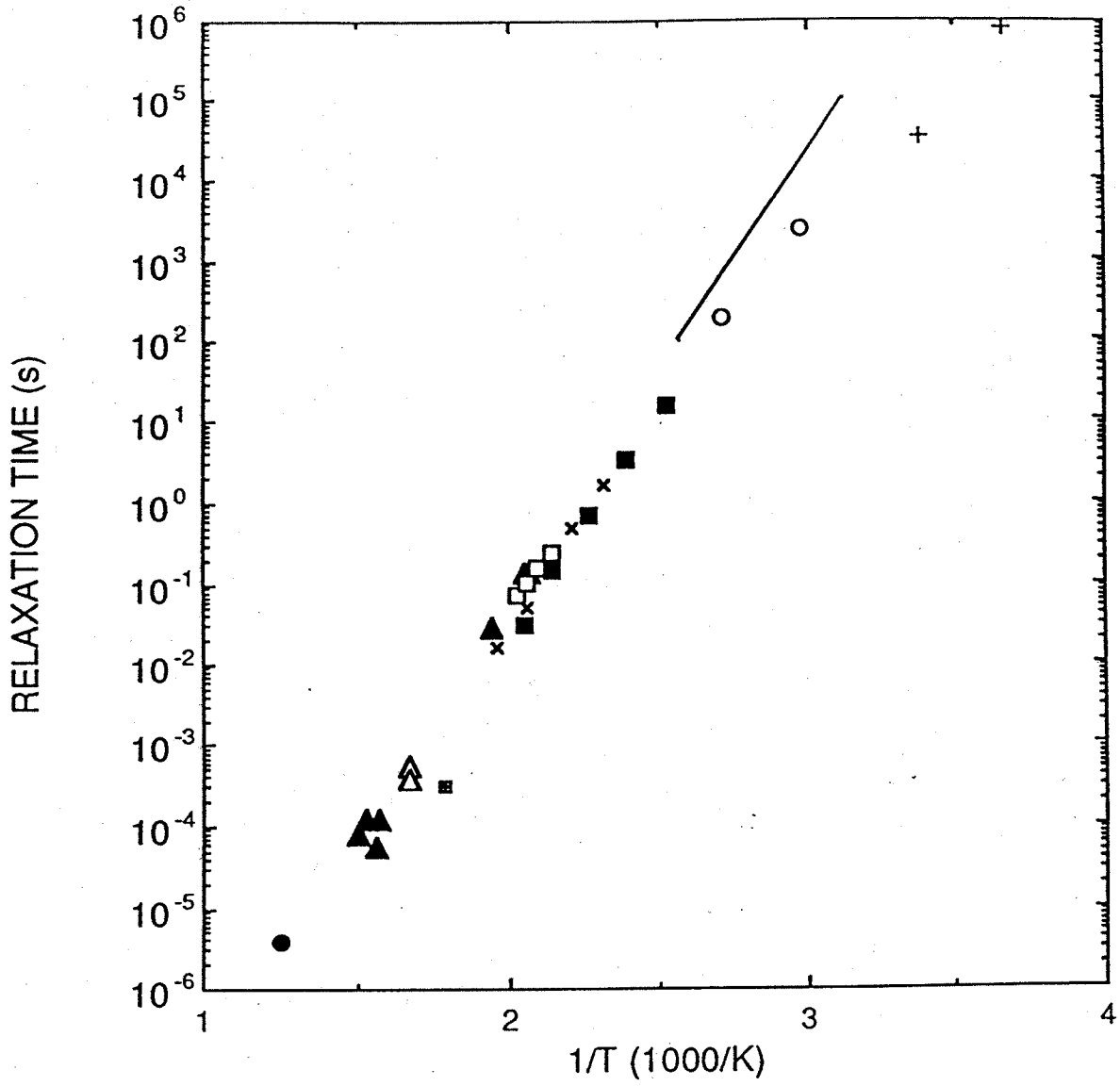


Figure 17. Relaxation time obtained from internal friction, anelastic relaxation, and time-dependent $T_c$ measurements vs 1/T. Data are from: filled circles,[62] crosses,[65] filled squares,[66] open triangles,[58] filled triangles,[7] open squares,[64] small filled square,[59] square cross,[70,71] and open circles.[69] The line is the fit to 26 data points from an anelastic relaxation experiment.[68]

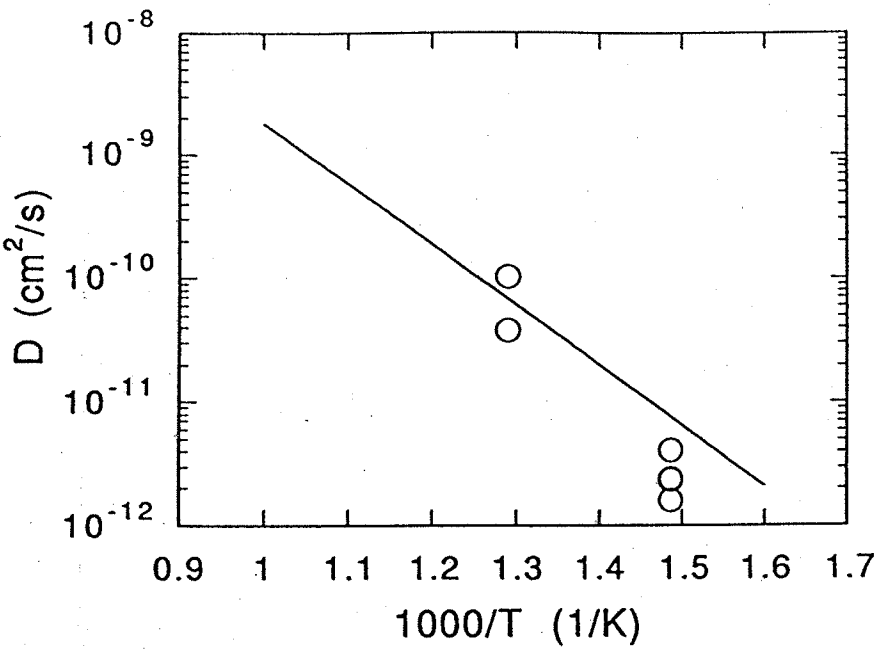


Figure 18. Arrhenius plot of the oxygen tracer diffusion coefficient measured in Nd-123 (open circles) compared to that obtained for Y-123 (solid line).[74]

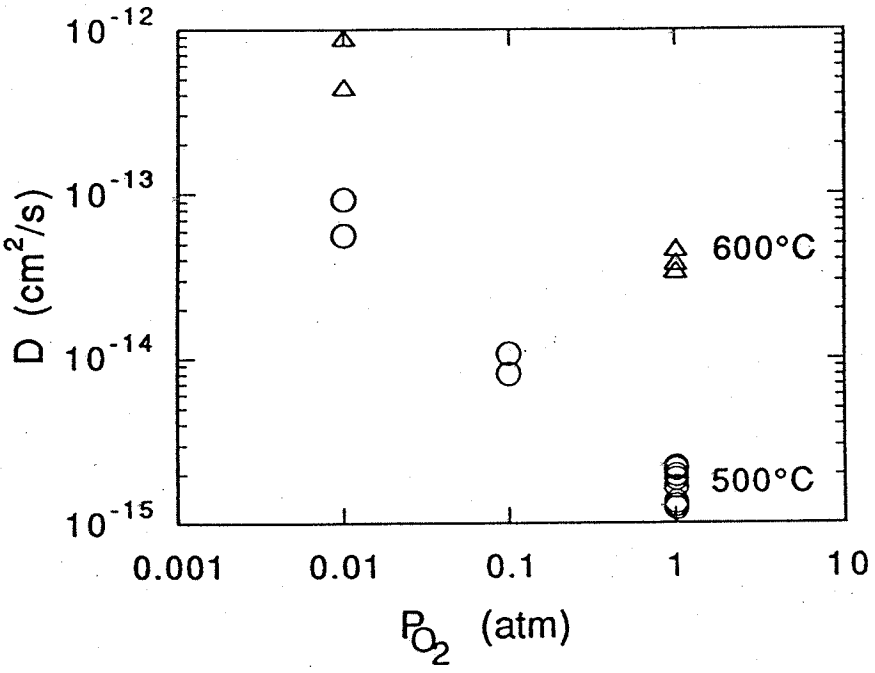


Figure 19. Variation of D at 500°C (circles) and 600°C (triangles) with oxygen partial pressure for $YBa_2Cu_4O_8$.[76]

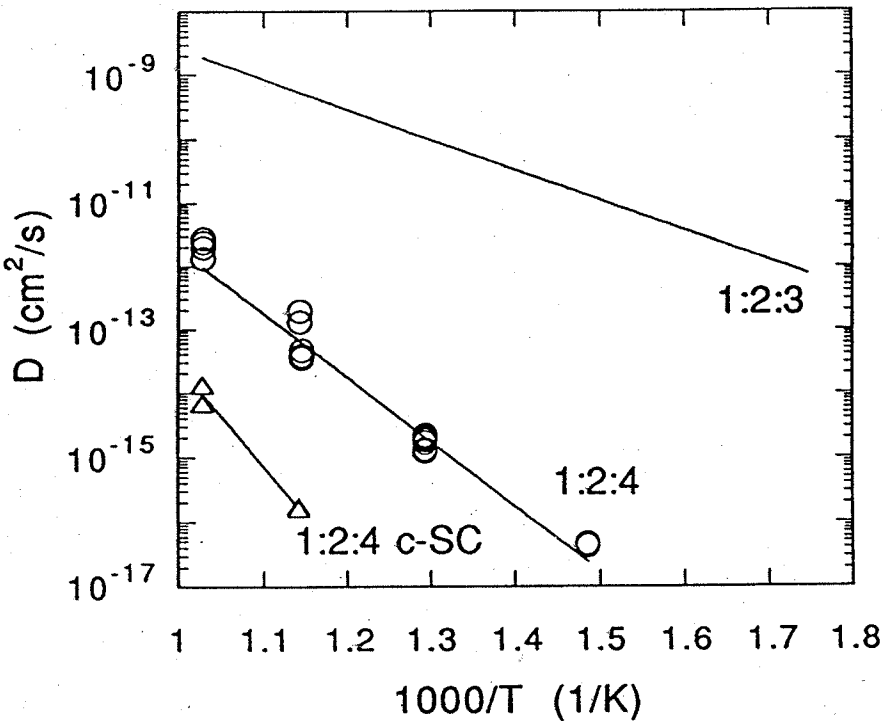


Figure 20. Arrhenius plot of oxygen diffusion data measured for polycrystalline Y 1:2:4 (circles) and c-axis single crystals (triangles) compared to polycrystaline Y 1:2:3.[9]

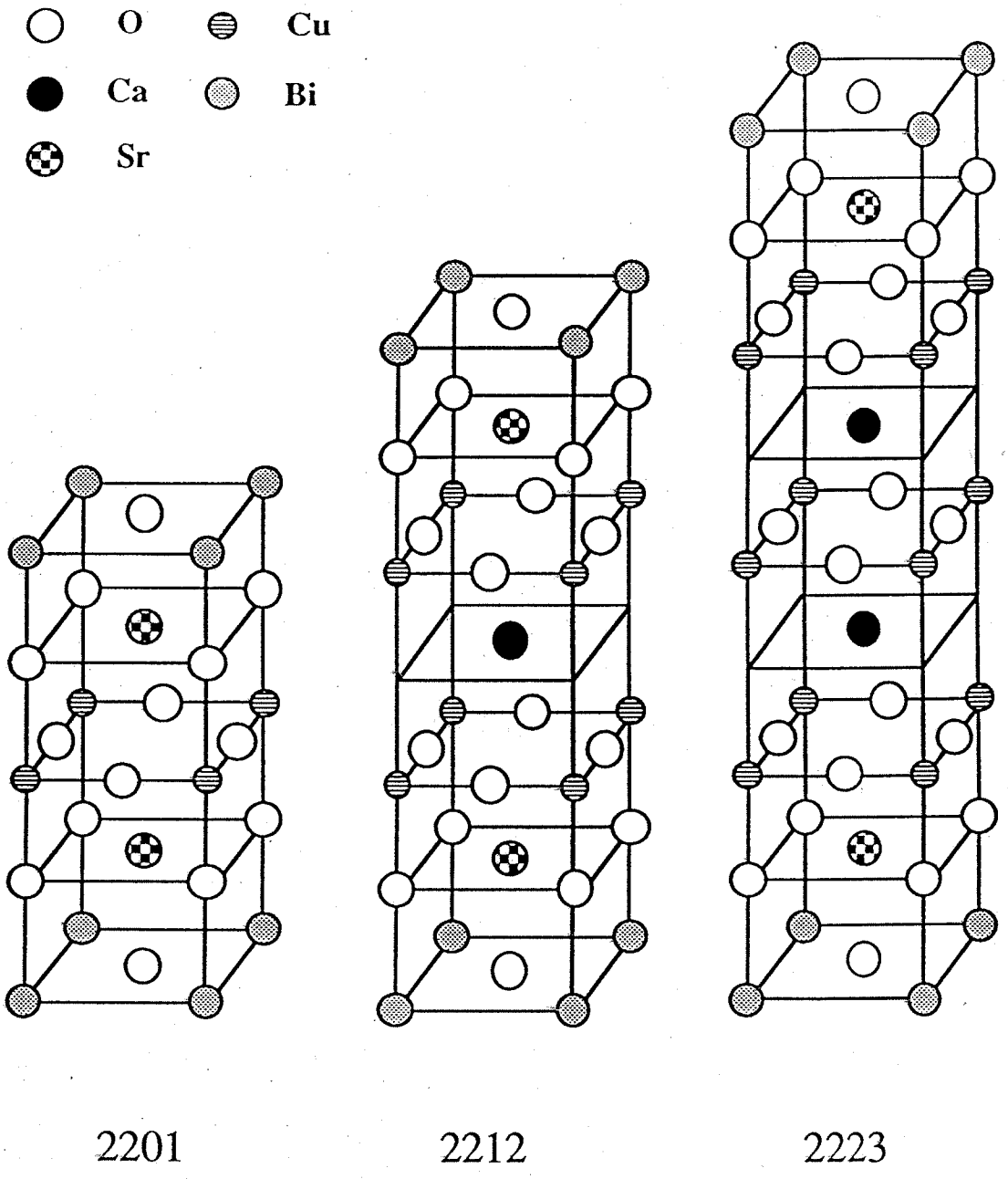


Figure 21. Structure of $Bi_2Sr_2Ca_{n-1}Cu_nO_{2n+4}$ for 2201 (n =1), 2212 (n = 2), and 2223 (n = 3).

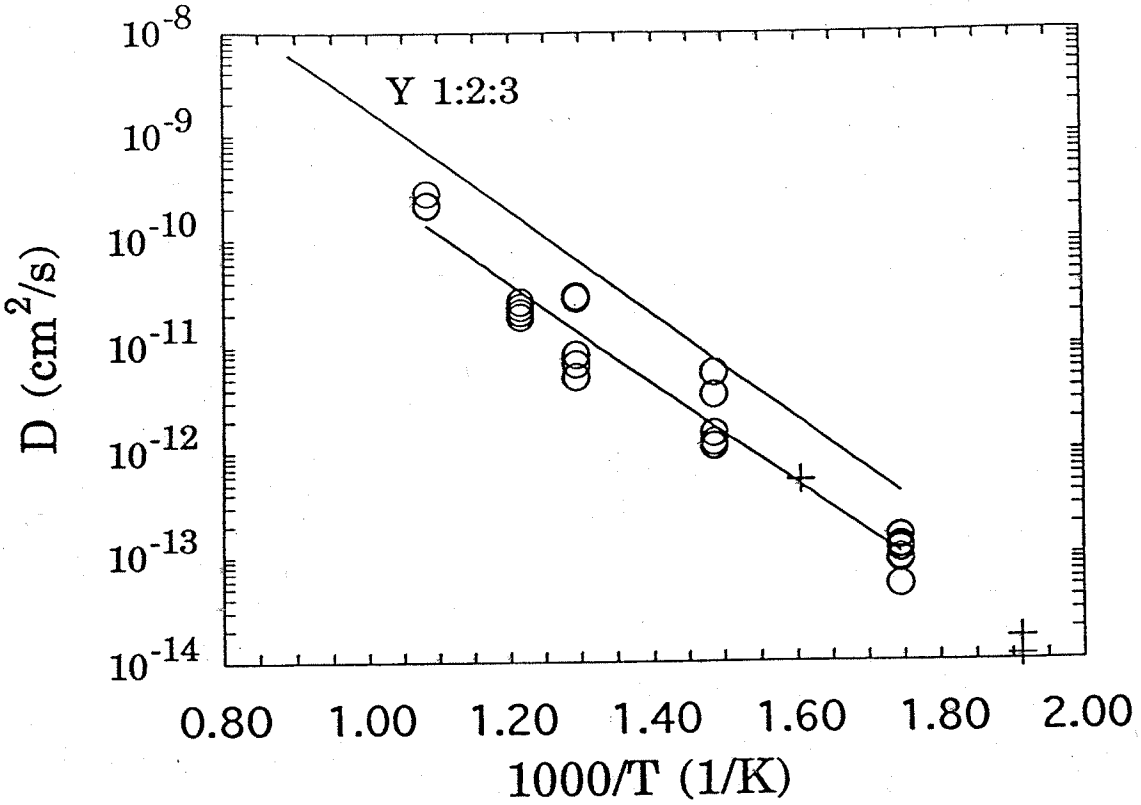


Figure 22. Arrhenius plot of the diffusion coefficients from oxygen tracer diffusion in polycrystalline $Bi_2Sr_2CaCu_2O_x$ (open circles),[84] compared to Y 1:2:3 polycrystals,[9] and parallel to the ab-plane in $Bi_2Sr_2CuO_x$ (crosses).[3]

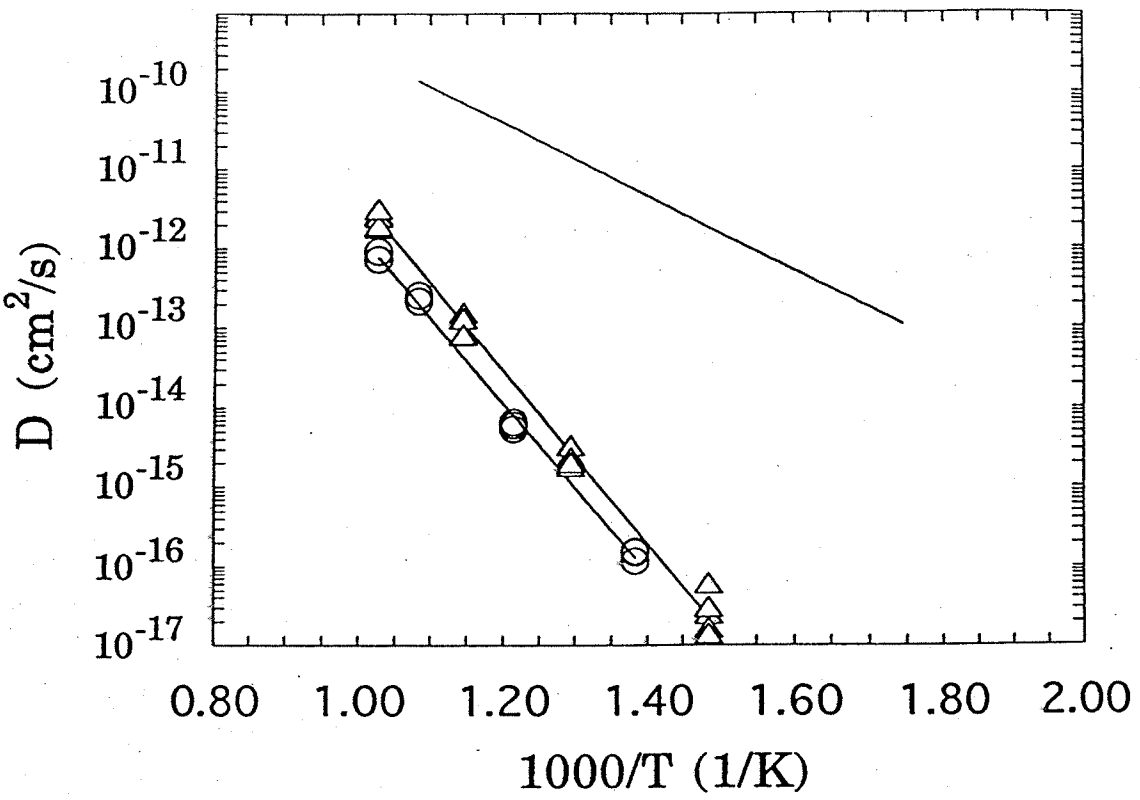


Figure 23. Arrhenius plot showing oxygen diffusion in the c direction in $Bi_2Sr_2CaCu_2O_x$ (triangles) and $Bi_2Sr_2CuO_x$ (circles) compared to diffusion in polycrystalline $Bi_2Sr_2CaCu_2O_x$ (solid line).[3,84]